Formation of Hydrogen Bonds in Complexes between Dimethylcuprate(I) Anion and Methane, Propane, or Dimethyl Ether. A Theoretical Study

Piotr I. Dem′yanov*,† and Ruth M. Gschwind*,‡

Chemistry Department, Moscow State University, Lenin Hills 1, Building 3, Moscow, 119992 GSP-2, Russian Federation, and Institut für Organische Chemie, Universität Regensburg, Universitätsstrasse 31, D-93053 Regensburg, Germany

Received May 12, 2006

Complexes of the neutral ligands methane, propane, and dimethyl ether (DME) with a dimethylcuprate-(I) anion (DMCA) were studied using B3LYP and MP2 methods. The quantum theory of atoms in molecule and the second-order perturbation natural bond orbital analysis were applied to analyze the electron density distributions of these complexes and to elucidate the nature of weak closed-shell interactions between the C−H bonds of the ligands and different atoms and bonds of DMCA. The presented results show that the copper center of DMCA interacts with the C−H bonds of methane, propane, and DME via formation of Cu···H−C hydrogen bonds, with the Cu center being an electron charge donor (hydrogen bond acceptor). The formation of weak dihydrogen bonds and C−H···C hydrogen bonds between C−H bonds of the neutral ligands and methyl groups of DMCA additionally stabilizes these complexes. Second-order orbital interactions of C−Cu bonds with C−H bonds contribute also to the formation of the complexes. Each of these interactions is very weak, but the sum of these interactions may have the potential to influence the structures of organocuprates(I), possessing very flat potential energy surfaces.

Introduction

The interaction of transition metals (TMs) with carbon−hydrogen (C−H) bonds is fundamentally important for C−H bond activation,[1] which plays a key role in heterogeneous and homogeneous hydrocarbon transformations.

In TM···H−C interactions, the interactions of orbitals of a TM atom with orbitals located on the C−H bond are of crucial importance. It is recognized now that metal atom orbitals exhibit amphoteric character.[2] This amphoteric behavior is reflected by the ability of TM atoms to accept electron density from and donate it to C−H or X−H bonds. Electron-deficient TMs, i.e., bare atoms of the left-hand side of the TM rows, bare cations, and atoms of cationic complexes tend to accept electron density from X−H bonds. The term agostic interaction was initially proposed for such intramolecular interactions of an electron-deficient TM with a C−H bond[3a] and then extended[3b] to both intramolecular and intermolecular interactions of TMs with X−H (X = C, B, N, Si) bonds. To emphasize the difference between intra- and intermolecular agostic interactions, the latter were suggested to be called pseudoagostic.[2] The very right-hand TMs and metal centers of electron-rich neutral and anionic complexes of other TMs are more prone to donate electron density to hydrogen-bond-donating X−H (X is an electronegative main group element, e.g., N, O, S) bonds to form X−H···TM hydrogen bonds[2,4] (HBs). The formation of C−H···TM HBs was also established.[2a,4e] Both agostic interactions and HBs can appreciably affect the structures[2b] and reactivities of organometallic compounds and TM complexes.

Cuprates(I) are well-known synthetic reagents broadly used in organic synthesis.[5] However, the existence of agostic interactions or hydrogen bonds in diorganocuprates(I) and organocop-

* To whom correspondence should be addressed. (P.I.D.) Phone: ++007 (495) 939 3565. Fax: ++007 (495) 939 5546. E-mail: pdem@org.chem.msu.ru. (R.M.G.) Phone: ++49 +941 943 4625. Fax: ++49 +941 943 4617. E-mail: ruth.gschwind@chemie.uni-regensburg.de.

† Moscow State University.

‡ Universität Regensburg.

(1) (a) Armentrout, P. B. In *Selective Hydrocarbon Activation: Principles and Progress*; Davies, J. A., Greenberg, A., Liebman, J. F., Eds.; VCH: New York, 1990; p 467. (b) Armentrout, P. B. *Annu. Rev. Phys. Chem.* **1990**, *41*, 313−344. (c) Weisshaar, J. C. *Adv. Chem. Phys.* **1992**, *82*, 213−262. (d) Weisshaar, J. C. *Acc. Chem. Res.* **1993**, *26*, 213−219. (e) Crabtree, R. H. *Chem. Rev.* **1985**, *85*, 245−269. (f) Crabtree, R. H. *Angew. Chem.* **1993**, *105*, 828−845; *Angew. Chem., Int. Ed. Engl.* **1993**, *32*, 789−805. (g) Shilov, A. E.; Shul′pin, G. B. *Chem. Rev.* **1997**, *97*, 2879−2932. (h) Kubas, G. J. *J. Organomet. Chem.* **2001**, *635*, 37−68. (i) Niu, S.; Hall, M. B. *Chem. Rev.* **2000**, *100*, 353−405. (j) Crabtree, R. H. *Dalton Trans.* **2001**, 2437−2450. (k) Labinger, J. A.; Bercaw, J. E. *Nature* **2002**, *417*, 507−514.

(2) (a) Braga, D.; Grepioni, F.; Tedesco, E.; Biradha, K.; Desiraju, G. R. *Organometallics* **1997**, *16*, 1846−1856. (b) Braga, L.; Grepioni, F.; Desiraju, G. R. *Chem. Rev.* **1998**, *98*, 1375−1405.

(3) (a) Brookhart, M.; Green, M. L. H. *J. Organomet. Chem.* **1983**, *250*, 395−408. (b) Brookhart, M.; Green, M. L. H.; Wong, L. L. *Progr. Inorg. Chem.* **1988**, *36*, 1−124.

(4) (a) Steiner, T. *Angew. Chem.* **2002**, *114*, 50−80; *Angew. Chem., Int. Ed.* **2002**, *41*, 48−76. (b) Brammer, L.; Charnock, J. M.; Goggin, P. L.; Goodfellow, R. J.; Orpen, A. G.; Koetzle, T. F. *J. Chem. Soc., Dalton Trans.* **1991**, 1789−1798. (c) Brammer, L.; Zhao, D.; Ladipo, F. T.; Braddoc-Wilking, J. *Acta Crystallogr.* **1995**, *B51*, 632−640. (d) Brammer, L. *Dalton Trans.* **2003**, 3145−3157. (e) Yao, W.; Eisenstein, O.; Crabtree, R. H. *Inorg. Chim. Acta* **1997**, *254*, 105−111. (f) Shubina, E. S.; Belkova, N. V.; Epstein, L. M. *J. Organomet. Chem.* **1997**, *536*−*537*, 17−29. (g) Epstein, L. M.; Shubina, E. S. *Coord. Chem. Rev.* **2002**, *231*, 165−181. (h) Martin, A. *J. Chem. Educ.* **1999**, *76*, 578−583. (i) Calhorda, M. J. *J. Chem. Soc., Chem. Commun.* **2000**, 801−809.

(5) (a) Lipshutz, B. H. In *Organometallics in Synthesis*; Schlosser, M., Ed.; Wiley: Chichester U.K., 1994; pp 283−382. (b) Taylor, R. J. K., Ed. *Organocopper Reagents: A practical approach*; Oxford University Press U.K.: Oxford, 1994. (c) Krause, N. *Metallorganische Chemie*; Spektrum Akademischer Verlag: Heidelberg, 1996. (d) Krause, N., Ed. *Modern Organocopper Chemistry*; Wiley-VCH: Weinheim, 2002. (e) van Koten, G.; James, S. L.; Jastrzebski, J. T. B. H. In *Comprehensive Organometallic Chemistry II*; Abel, E. W., Stone, F. G. A., Wilkinson, G., Eds.; Pergamon: Oxford, 1995; Vol. 3, pp 57−133. (f) Nakamura, E.; Mori, S. *Angew. Chem.* **2000**, *112*, 3902−3924; *Angew. Chem., Int. Ed.* **2000**, *39*, 3750−3771.

10.1021/om0604066 CCC: $33.50
Publication on Web 10/19/2006

per(I) compounds has never been discussed or even proposed up to now. The only exceptions are two weak association complexes of a dimethylcuprate(I) anion (DMCA) with dimethyl ether (DME), $(Me_2Cu)^-\cdots HCH_2OCH_3$, localized by the B3LYP calculations of Mori et al.[6] The authors found that these weak complexes did not affect the activation energy of the reaction studied and stated that the copper atom in lithium organocuprates(I) does not accept any neutral ligand. They argued that this conclusion is supported by a lack of coordination of neutral ligands to copper centers in lithium organocuprate(I) structures deposited in the Cambridge Structural Database[7] (CSD) or described in the existing reviews.

Nevertheless, a very close contact of 2.23 Å between copper and an H atom of norbornene was found in a solid norbornene-(diethylenetriamine)copper(I) tetraphenylborate as early as 1978.[8] The close C−H···TM contacts in Cu(I) and Cu(II) complexes with organic ligands were also found[2] in structures deposited in the CSD. Agostic interactions were revealed in copper(I) complexes with X−H (X = C, Si, Ge) bonds of saturated and unsaturated alkanes, silanes, and germanes[9a,b] and XH_3 (X = B, Al, Ga) molecules.[9c] A strong interaction of C−H bonds of ethane with Cu^+ ions in Cu(I)−ZSM-5 zeolite was recently described.[10] A short distance (2.454 Å) between the C−H bond and the copper atom in the Cu(II) complex with chiral ephedrine was recently found.[11] This C−H···Cu interaction, initially referred to as an agostic interaction,[11] was recently reassessed as a weak intramolecular hydrogen bond formed by the C−H bond with two acceptors, namely, Cu(II) and the carboxylate oxygen atom.[12] It is proposed[11] that C−H···Cu close contacts can affect the stereocontrol in catalytic reactions with Cu(II) as catalyst.

On account of the described copper-ligand interactions and their impact on structures and reactivities, in this study the kind and strength of intermolecular interactions between diorganocuprate(I) anions and neutral ligands or solvent molecules were reinvestigated using the density functional theory[13] (DFT), the second-order Møller−Plesset (MP2) perturbation theory,[14] the quantum theory of atoms in molecules (QTAIM),[15] and the natural bond orbital (NBO) analysis. The complexes between dimethylcuprate(I) anion and methane, propane, or dimethyl ether are chosen as model systems. Different types of hydrogen bonds between DMCA and C−H bonds of these ligands are predicted to occur, Cu···H−C hydrogen bonds being the most interesting among those. The second-order orbital interactions of C−Cu bonds with C−H bonds of the ligands studied contribute also to the formation of complexes. Although the strength of each of the predicted characteristic interactions is very weak, in total they should be able to influence the highly flexible aggregate structures of diorganocuprates(I) and their reactivity.

Computational Details

The calculations were carried out with the Gaussian 98[16] (G98) and Gaussian 03[17] (G03) quantum chemistry software packages. The geometries of the studied molecules were completely optimized at the B3LYP[18] and MP2[14] theory levels. Core electrons were not included in the correlation treatment with MP2 calculations, i.e., the MP2 frozen core (FC) method was explored. Ahlrichs SVP[19] all-electron basis set for Cu together with 6-31G(d) or with 6-31G-(2df,p) basis sets for the rest (hereafter referred to as basis set I and II, respectively) were used for the majority of optimizations. It is to be noted that the B3LYP/I method is explored intensively by Nakamura et al.[5f,6,20] for the theoretical study on structures and reactivities of organocuprate(I) and organocopper(III) species. It was shown[20h,21] that B3LYP/I calculations give structures and energetics for organocopper(I) species almost identical to those obtained using the SDD basis set with Stuttdgardt's quasirelativistic effective core pseudopotential (ECP) for copper or the data obtained by the CCSD(T) calculations. The 6-31G(2df,p) basis was recommended for geometry optimization and zero point energy (ZPE) calculation in the frame of G3X theory.[22] DMCA and its complex with methane were also optimized using the B3LYP and MP2-

(6) Mori, S.; Nakamura, E.; Morokuma, K. *J. Am. Chem. Soc.* **2000**, *122*, 7294−7307.
(7) Allen, F. H. *Acta Crystallogr.* **2002**, *B58*, 380−388.
(8) Pasqualli, M.; Floriani, C.; Gaetani-Manfredotti, A.; Chiesi-Villa, A. *J. Am. Chem. Soc.* **1978**, *100*, 4918−4919.
(9) (a) Corral, I.; Mó, O.; Yáñez, M. *J. Phys. Chem. A* **2003**, *107*, 1370−1376. (b) Corral, I.; Mó, O.; Yáñez, M. *Int. J. Mass Spectrom.* **2003**, *227*, 401−412. (c) Corral, I.; Mó, O.; Yáñez, M. *Int. J. Quantum Chem.* **2006**, *106*, 659−663.
(10) Pidko, E.; Kazansky, V. *Phys. Chem. Chem. Phys.* **2005**, *7*, 1939−1944.
(11) Castro, M.; Cruz, J.; López-Sandoval, H.; Barba-Behrens, N. *Chem. Commun.* **2005**, 3779−3781.
(12) Thakur, T. S.; Desiraju, G. R. *Chem. Commun.* **2006**, 552−554.
(13) (a) Hohenberg, P.; Kohn, W. *Phys. Rev. B* **1964**, *136*, 864−871. (b) Kohn, W.; Sham, L. J. *J. Phys. Rev. A* **1965**, *140*, 1133−1138. (c) Parr, R. G.; Yang, W. *Density-Functional Theory of Atoms and Molecules*; Oxford University Press: Oxford, 1989.
(14) Møller, C.; Plesset, M. S. *Phys. Rev.* **1934**, *46*, 618−622.
(15) Bader, R. F. W. *Atoms in Molecules. A Quantum Theory*; Clarendon Press: Oxford, 1994.
(16) Frisch, M. J.; Trucks, G. W.; Schlegel, H. B.; Scuseria, G. E.; Robb, M. A.; Cheeseman, J. R.; Zakrzewski, V. G.; Montgomery, J. A., Jr.; Stratmann, R. E.; Burant, J. C.; Dapprich, S.; Millam, J. M.; Daniels, A. D.; Kudin, K. N.; Strain, M. C.; Farkas, O.; Tomasi, J.; Barone, V.; Cossi, M.; Cammi, R.; Mennucci, B.; Pomelli, C.; Adamo, C.; Clifford, S.; Ochterski, J.; Petersson, G. A.; Ayala, P. Y.; Cui, Q.; Morokuma, K.; Malick, D. K.; Rabuck, A. D.; Raghavachari, K.; Foresman, J. B.; Cioslowski, J.; Ortiz, J. V.; Baboul, A. G.; Stefanov, B. B.; Liu, G.; Liashenko, A.; Piskorz, P.; Komaromi, I.; Gomperts, R.; Martin, R. L.; Fox, D. J.; Keith, T.; Al-Laham, M. A.; Peng, C. Y.; Nanayakkara, A.; Challacombe, M.; Gill, P. M. W.; Johnson, B.; Chen, W.; Wong, M. W.; Andres, J. L.; Gonzalez, C.; Head-Gordon, M.; Replogle, E. S.; Pople, J. A. *Gaussian 98*, revision A.9; Gaussian, Inc.: Pittsburgh, PA, 1998.
(17) Frisch, M. J.; Trucks, G. W.; Schlegel, H. B.; Scuseria, G. E.; Robb, M. A.; Cheeseman, J. R.; Montgomery, J. A., Jr.; Vreven, T.; Kudin, K. N.; Burant, J. C.; Millam, J. M.; Iyengar, S. S.; Tomasi, J.; Barone, V.; Mennucci, B.; Cossi, M.; Scalmani, G.; Rega, N.; Petersson, G. A.; Nakatsuji, H.; Hada, M.; Ehara, M.; Toyota, K.; Fukuda, R.; Hasegawa, J.; Ishida, M.; Nakajima, T.; Honda, Y.; Kitao, O.; Nakai, H.; Klene, M.; Li, X.; Knox, J. E.; Hratchian, H. P.; Cross, J. B.; Adamo, C.; Jaramillo, J.; Gomperts, R.; Stratmann, R. E.; Yazyev, O.; Austin, A. J.; Cammi, R.; Pomelli, C.; Ochterski, J. W.; Ayala, P. Y.; Morokuma, K.; Voth, G. A.; Salvador, P.; Dannenberg, J. J.; Zakrzewski, V. G.; Dapprich, S.; Daniels, A. D.; Strain, M. C.; Farkas, O.; Malick, D. K.; Rabuck, A. D.; Raghavachari, K.; Foresman, J. B.; Ortiz, J. V.; Cui, Q.; Baboul, A. G.; Clifford, S.; Cioslowski, J.; Stefanov, B. B.; Liu, G.; Liashenko, A.; Piskorz, P.; Komaromi, I.; Martin, R. L.; Fox, D. J.; Keith, T.; Al-Laham, M. A.; Peng, C. Y.; Nanayakkara, A.; Challacombe, M.; Gill, P. M. W.; Johnson, B.; Chen, W.; Wong, M. W.; Gonzalez, C.; Pople, J. A. *Gaussian 03*, revision B.03; Gaussian, Inc.: Pittsburgh, PA, 2003.
(18) (a) Becke, A. D. *Phys. Rev. A* **1988**, *38*, 3098−3100. (b) Becke, A. D. *J. Chem. Phys.* **1993**, *98*, 5648−5652. (c) Lee, C.; Yang, W.; Parr, R. G. *Phys. Rev. B* **1988**, *37*, 785−789.
(19) Schäfer, A.; Horn, H.; Ahlrichs, R. *J. Chem. Phys.* **1992**, *97*, 2571−2577.
(20) (a) Nakamura, E.; Mori, S.; Nakamura, M.; Morokuma, K. *J. Am. Chem. Soc.* **1997**, *119*, 4887−4899. (b) Nakamura, E.; Mori, S.; Morokuma, K. *J. Am. Chem. Soc.* **1997**, *119*, 4900−4910. (c) Mori, S.; Nakamura, E. In *Modern Organocopper Chemistry*; Krause, N., Ed.; Wiley-VCH: Weinheim, 2002; pp 315−346. (d) Mori, S.; Nakamura, E. *Eur. J. Chem.* **1999**, *5*, 1534−1543. (e) Yamanaka, M.; Nakamura, E. *Organometallics* **2001**, *20*, 5675−5681. (f) Yamanaka, M.; Inagaki, A.; Nakamura, E. *J. Comput. Chem.* **2003**, *24*, 1401−1409. (g) Nakamura, E.; Yoshikai, N. *Bull. Chem. Soc. Jpn.* **2004**, *77*, 1−12. (h) Yamanaka, M.; Kato, S.; Nakamura, E. *J. Am. Chem. Soc.* **2004**, *126*, 6287−6293. (i) Yamanaka, M.; Nakamura, E. *J. Am. Chem. Soc.* **2005**, *127*, 4697−4706.
(21) Nakanishi, W.; Yamanaka, M.; Nakamura, E. *J. Am. Chem. Soc.* **2005**, *127*, 1446−1453.
(22) Curtiss, L. A.; Redfern, P. C.; Raghavachari, K.; Pople, J. A. *J. Chem. Phys.* **2001**, *114*, 108−117.

(FC) methods together with the 6-311++G(2d,2p) basis for C and H, while the small core quasi-relativistic effective SDD pseudopotential of the Stuttgardt group[23] and the contracted scalar relativistic 19 valence electron basis set[24] were explored for Cu. This basis set is hereafter designated as basis III. Target molecules were also optimized without any constraints using for all atoms the large and flexible 6-311++G(3df,3pd) basis set (denoted as XL) stored internally in the G98 and G03 packages. The basis set XL was also used for calculations of energies for both B3LYP/I- and B3LYP/II-optimized species, while the energies of B3LYP/III- and MP2(FC)/III-optimized species were also calculated using 6-311++G(2d,2p) for C and H and quadruple-ζ valence basis combined with the PP set of polarization functions (QZVPP)[25] for Cu. The last composite basis is henceforth denoted as basis IV. Ahlrichs SVP[19] all-electron basis set for Cu was used in this work instead of SDD or other ECP-based basis sets to avoid complications[26] in the topological analysis of B3LYP/I- and B3LYP/II-calculated species in the frame of QTAIM.[15] For the same reason the QZVPP all-electron basis set (without g functions)[27] for Cu was explored to obtain wave functions for B3LYP/III- and MP2-(FC)/III-calculated species. The lack of g functions has practically no effect on the energy and other properties of the molecule.[25a] Thus, the energy of the B3LYP-calculated DMCA−methane complex increases by 0.013 kcal/mol only if both g functions are removed from the QZVPP basis. The Molden 3.7[28] program was applied for a visualization of molecular orbitals.

All stationary points located on potential energy surfaces (PESs) were obtained without any symmetry assumptions and characterized by vibrational frequencies calculated at the corresponding theory level. All optimized structures correspond to energy minima because no imaginary frequencies were found. The dissociation energies of complexes into the isolated DMCA and neutral ligand were corrected for ZPE to give $E°$ values. Scale factors of 0.9806,[29] 0.9854,[22] and 0.9670[29] were used for B3LYP/I-, B3LYP/II-, and MP2(FC)/I-calculated ZPEs, respectively. The B3LYP/III-, B3LYP/XL-, MP2(FC)/II-, and MP2(FC)/III-calculated ZPEs were explored without corrections, since there are no scale factors well documented for these methods. MP2(FC)/III- and B3LYP/III-calculated ZPEs were also used for MP2/IV//MP2/III and B3LYP/IV//B3LYP/III calculations of dissociation energies, respectively. The basis set superposition error (BSSE)[30] corrections for $E°$ were computed using the counterpoise method of Boys and Bernardi.[31] The standard procedure ("counterpoise=2" option) of G03 was explored to calculate the BSSE.

The NBO Version 3.1 program[32] implemented in the G03 package was used for natural atomic orbital, natural bond orbital, and the second-order perturbation NBO analysis. QTAIM analysis[15] of B3LYP- and MP2-calculated electron density distributions in the molecules optimized in this work was performed using the AIM2000 program.[33] G98 and G03 failed to give B3LYP/XL wave functions presumably because the XL basis contains a g function on Cu. Therefore the topological analysis for B3LYP/XL-optimized complexes was not performed.

Results and Discussion

B3LYP and MP2 optimizations of the bare DMCA, $(Me_2Cu)^-$, were carried out using basis sets I, II, and XL. Also basis III was explored to take into account relativistic effects, which can potentially affect the structure of copper compounds.[34] Both B3LYP and MP2 calculations of the DMCA lead to the linear anion **1** with eclipsed methyl groups (Figure 1). All B3LYP calculations underestimate carbon−copper interactions in **1** and result in sufficiently longer Cu−C bonds (Tables 1 and 2) compared with those X-ray measured in solvent-separated ion pairs (SSIPs) of DMCA.[35] It is important to note that the relativistic B3LYP/III calculation yields the same Cu−C bond length (d(Cu−C)) as the nonrelativistic B3LYP/II optimization, whereas the extralarge XL basis leads to even larger d(Cu−C). On the other hand, for **1** B3LYP optimization with the smallest basis I gives results that are closer to B3LYP/II and B3LYP/III results. At the same time, the relativistic MP2/III calculation predicts (Table 2) too short Cu−C bonds for **1**, whereas the nonrelativistic MP2/II optimization gives the best estimation of d(Cu−C) in that anion.

B3LYP and MP2 calculations show that an interaction of DMCA with methane results in complexes **2**. Molecular graphs for B3LYP/II-, B3LYP/III-, MP2/II-, and MP2/III-optimized DMCA−methane complexes, described by B3LYP/II (**2a**), B3LYP/IV (**2b**), MP2/II (**2c**), and MP2/IV (**2d**) wave functions, respectively, exemplify the structures of these complexes (Figure 1). The uncorrected for BSSE dissociation energy ($E°$) of **2** is positive at all theory levels used (Table 3), demonstrating that **2** is stable with respect to the separated **1** and methane. However, the counterpoise-corrected dissociation energies (E^{CP}) calculated using basis sets I and II are negative (Table 3). The counterpoise correction often results, however, in overestimated BSSEs and thus underestimates the binding energies compared to experimental values.[36] In such cases it is recommended to employ a 50% BSSE correction.[36a,37] Notably, B3LYP/I- and B3LYP/II-calculated E^{CP}'s are also positive (0.37 and 0.40 kcal/mol, respectively) with 50% BSSE corrections. Using larger basis sets for the optimization and the energy calculation gives small but positive $E°$ and E^{CP} energies, demonstrating that an interaction of DMCA with methane results in a stable complex. It is worth noticing that the dissociation energies, calculated using the B3LYP functional with relativistic basis III and nonrelativistic basis sets IV and XL, are close to each other. MP2 calculations predict a similar picture (Table 3). However, MP2-calculated E^{CP}'s exceed the B3LYP-calculated E^{CP}'s by more than 2 times. Significantly larger MP2-calculated binding energies compared with those predicted by B3LYP were also

(23) Dolg, M.; Wedig, U.; Stoll, H.; Preuss, H. *J. Chem. Phys.* **1987**, *86*, 866−872.
(24) Hermann, H. L.; Boche, G.; Schwerdtfeger, P. *Chem. Eur. J.* **2001**, *7*, 5333−5342.
(25) (a) Weigend, F.; Furche, F.; Ahlrichs, R. *J. Chem. Phys.* **2003**, *119*, 12753−12762. (b) Weigend, F.; Ahlrichs, R. *Phys. Chem. Chem. Phys.* **2005**, *7*, 3297−3305.
(26) (a) Vyboishchikov, S. F.; Sierraalta, A.; Frenking, G. *J. Comput. Chem.* **1997**, *18*, 416−429. (b) Macchi, P.; Sironi, A. *Coord. Chem. Rev.* **2003**, *238−239*, 383−412, and references therein.
(27) G98 and G03 failed to give files of wave functions required for QTAIM analyses if the full QZVPP basis was used.
(28) Schaftenaar, G. The CMBI at the University of Nijmegen, The Netherlands (http://www.cmbi.kun.nl/~schaft/molden).
(29) Scott, A. P.; Radom, L. *J. Phys. Chem.* **1996**, *100*, 16502−16513.
(30) van Duijneveldt, F. B.; van Duijneveldt-van de Rijdt, J. G. C. M.; van Lenthe, J. H. *Chem. Rev.* **1994**, *94*, 1873−1885.
(31) Boys, S. F.; Bernardi, F. *Mol. Phys.* **1970**, *19*, 553−566.
(32) Reed, A. E.; Curtiss, L. A.; Weinhold, F. *Chem. Rev.* **1988**, *88*, 899−926.
(33) Biegler-König, F.; Schönbohm, J.; Bayles, D. J. *J. Comput. Chem.* **2001**, *22*, 545−559.
(34) Pyykkö, P. *Chem. Rev.* **1988**, *88*, 563−594.
(35) (a) Hope, H.; Olmsted, M. M.; Power, P. P.; Sandell, J.; Xu, X. *J. Am. Chem. Soc.* **1985**, *107*, 4337−4338. (b) John, M.; Auel, C.; Behrens, C.; Marsch, M.; Harms, K.; Bosold, F.; Gschwind, R. M.; Rajamohanan, P. R.; Boche, G. *Chem. Eur. J.* **2000**, *6*, 3060−3068.
(36) (a) Kim, K. S.; Tarakeshwar, P.; Lee, J. Y. *Chem. Rev.* **2000**, *100*, 4145−4186, and referances therein. (b) Tarakeshwar, P.; Choi, H. S.; Kim, K. S. *J. Am. Chem. Soc.* **2001**, *123*, 3323−3331. (c) Zhao, Y.; Schultz, N. E.; Truhlar, D. G. *J. Chem. Phys.* **2005**, *123*, 1611031−1611034.
(37) (a) Chandra, A. K.; Zeegers-Huyskens, T. *J. Phys. Chem. A* **2005**, *109*, 12006−12013. (b) Singh, P. C.; Patwari, G. N. *Chem. Phys. Lett.* **2006**, *419*, 5−9. (c) Singh, P. C.; Patwari, G. N. *Chem. Phys. Lett.* **2006**, *419*, 265−268.

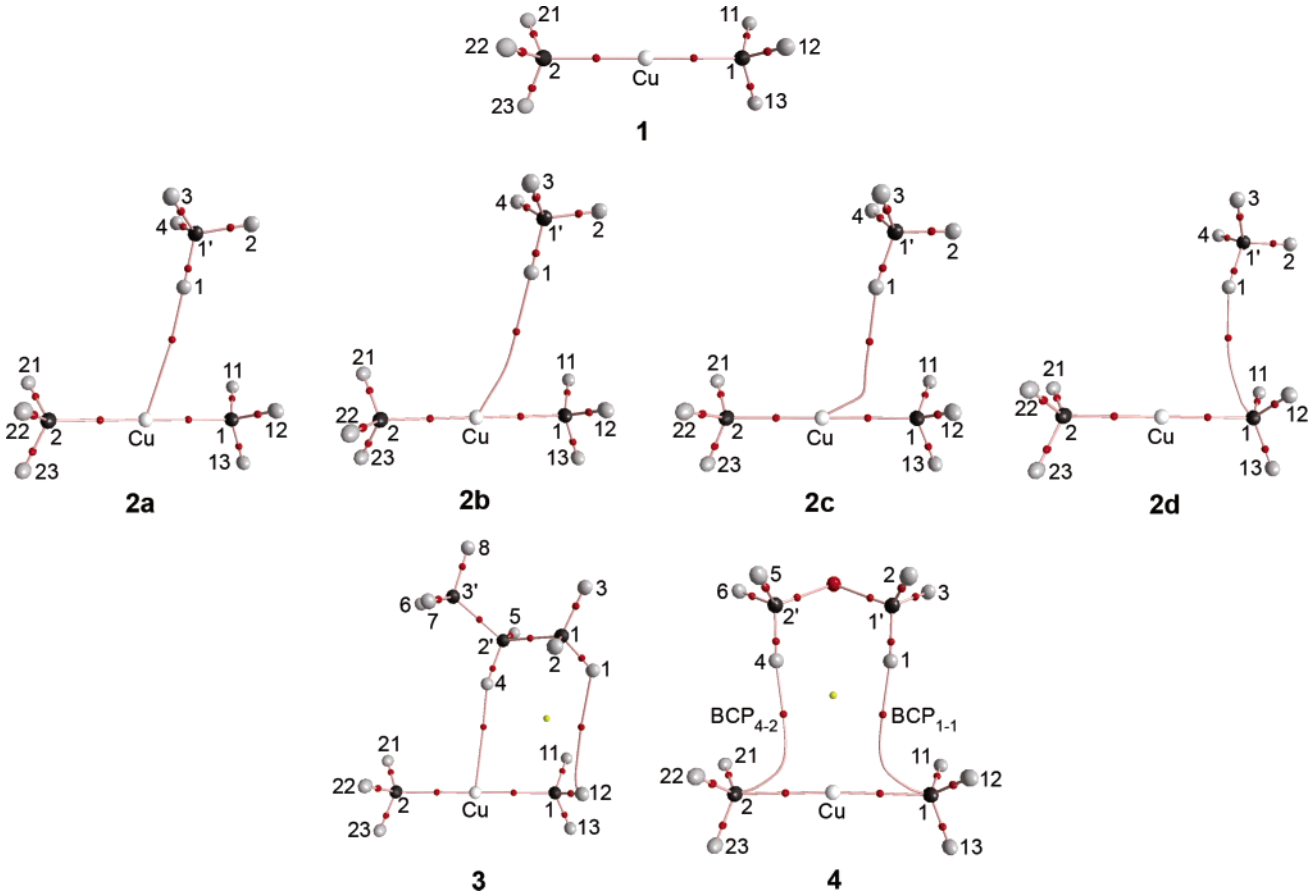

Figure 1. Molecular graphs for the dimethylcuprate(I) anion **1** and its complexes with methane (**2**), propane (**3**), and DME (**4**). The black, gray, and red spheres are carbon, hydrogen, and oxygen atoms, and small red and yellow spheres are (3,−1) bond critical points and (3,+1) ring critical points, respectively

found for methane−nitric oxide complexes,[38a] a very weak methane−water complex,[38b] and dimeric complexes such as methane dimer, ammonia dimer, water dimer, $H_2O\cdot(NH_3)$, $CH_4\cdot(NH_3)$, and $(FHF)^-$.[39] At the same basis set, MP2-calculated BSSEs are also much larger than B3LYP-predicted ones. That result agrees with the existing data on a sufficiently lower sensitivity of DFT calculations to the BSSE compared with methods taking electron correlations into account.[38,40] As a whole, B3LYP-calculated E^{CP} values for **2** are about 6 and 3 times lower than B3LYP/6-311++(2df,p)-calculated dissociation energies (with 50% BSSE) for complexes of methane with methyl and dichloromethyl carbanions, respectively.[37a] On the other hand, E^{CP}'s calculated for **2** using MP2 methods are comparable with the B3LYP-calculated dissociation energy of the $CH_4-(CHCl_2)^-$ complex.[37a] As the dissociation energies of hydrogen-bonded complexes for a given proton donor are correlated with the proton affinities of the bases,[37a] the comparisons described show that proton acceptor ability of a sufficiently delocalized DMCA is noticeably lower than that of methyl carbanion and comparable with the proton acceptor ability of dichloromethyl carbanion. This conclusion is quite expected.

MP2/III theory predicts for **2** shorter distances between the atoms of DMCA and methane, namely, *d*(Cu···H1) and *d*(C1···H1) distances (3.086 and 2.824 Å, respectively), compared with those predicted by B3LYP/III (3.222 and 3.226 Å, respectively) (Table 2). One could propose that larger separations in the second case are presumably because B3LYP overestimates the repulsion interaction of closed shells of the neutral molecule of methane and negatively charged DMCA and, as a result, provides too low interaction energies. Indeed, it is well known that B3LYP as well as other current DFT methods are often not able to describe correctly the dispersion interactions.[38,39,40b,41] On the other hand, B3LYP/I and B3LYP/II methods give shorter Cu···H1 separation (2.850 and 2.835 Å, respectively) than MP2/II theory (2.865 Å), while the C1···H1 distance predicted by the first two methods (3.125 and 3.096 Å, respectively) exceeds that of 2.817 Å calculated using MP2/II. The data obtained show that both B3LYP and MP2 methods lead to a strengthening of the interaction of methane with the C1-methyl group of DMCA and to a weakening of the interaction with Cu on the extension of the basis set and, as a

(38) (a) Crespo-Otero, R.; Montero, L. A.; Stohrer, W.-D.; García de la Vega, J. M. *J. Chem. Phys.* **2005**, *123*, 1341071−1341078. (b) Novoa, J. J.; Sosa, C. *J. Phys. Chem.* **1995**, *99*, 15837−15845.

(39) Rappé, A. K.; Bernstein, E. R. *J. Phys. Chem. A* **2000**, *104*, 6117−6128.

(40) (a) Simon, S.; Bertran, J.; Sodupe, M. *J. Phys. Chem. A* **2001**, *105*, 4359−4364. (b) Zhechkov, L.; Heine, T.; Patchkovskii, S.; Seifert, G.; Duarte, H. A. *J. Chem. Theory Comput.* **2005**, *1*, 841−847.

(41) (a) Kristyán, S.; Pulay, P. *Chem. Phys. Lett.* **1994**, *229*, 175−180. (b) Hobza, P.; Sponer, J.; Reschel, T. *J. Comput. Chem.* **1995**, *16*, 1315−1325. (c) Tsuzuki, S.; Uchimaru, T.; Tanabe, K. *Chem. Phys. Lett.* **1998**, *287*, 202−208. (d) Müller-Dethlefs, K.; Hobza, P. *Chem. Rev.* **2000**, *100*, 143−167. (e) Tsuzuki, S.; Lüthi, H. P. *J. Chem. Phys.* **2001**, *114*, 3949−3957. (f) Koch, W.; Holthausen, M. C. *A Chemist's Guide to Density Functional Theory*, 2nd ed.; Wiley-VCH: Weinheim, 2001; Chapter 12. (g) Johnson, E. R.; Wolkow, R. A.; DiLabio, G. A. *Chem. Phys. Lett.* **2004**, *394*, 334−338. (h) Hyla-Kryspin, I.; Haufe, G.; Grimme, S. *Chem. Eur. J.* **2004**, *10*, 3411−3422. (i) Zhao, Y.; Truhlar, D. G. *J. Phys. Chem. A* **2004**, *108*, 6908−6918. (j) Černý, J.; Hobza, P. *Phys. Chem. Chem. Phys.* **2005**, *7*, 1624−1626. (k) Zhao, Y.; Truhlar, D. G. *J. Chem. Theory Comput.* **2005**, *1*, 415−432. (l) Meier, R. J. *Chem. Phys. Lett.* **2005**, *401*, 594. (m) Koné, M.; Illien, B.; Graton, J.; Laurence, C. *J. Phys. Chem. A* **2005**, *109*, 11907−11913.

Table 1. Selected Internuclear Distances (Å), Bond Path Lengths (Å) in Parentheses, and Bond Angles (φ, deg) for B3LYP-Optimized Dimethylcuprate(I) Anion and Its Complexes with Neutral Ligands

molecule	parameter	B3LYP/I	B3LYP/II	B3LYP/XL
$(Me_2Cu)^-$, **1**	Cu−C1, Cu−C2	1.970, 1.971[a]	1.966, 1.935,[b] 1.929,[c] 1.937,[c] 1.963,[d]	1.981
	C1−H, C2−H	1.106	1.105	1.100
	C1−Cu−C2[e]	180.0	180.0, 180[a−d]	180.0
$(Me_2Cu\cdots H-CH_3)^-$, **2**	C1−Cu, C2−Cu	1.970	1.966	1.982
	Cu−H1	2.850 (2.875)	2.835 (2.862)	3.197
	C1−H1	3.125	3.096	3.158
	C1′−H1	1.095	1.094	1.089
	C1′−H2	1.095	1.093	1.089
	C1′−H3, C1′−H4	1.095	1.094	1.089
	C1−Cu−C2[e]	180.3	180.3	180.3
	H1−Cu−C1	78.5	78.0	70.8
$[Me_2Cu\cdots H_2C(Me)_2]^-$, **3**	C1−Cu		1.967 (1.967)	1.981
	C2−Cu		1.964 (1.964)	1.980
	Cu−H4		2.717 (2.738)	3.012
	C1−H4		3.176	3.081
	H1−H12		2.729 (2.929)	3.137
	C2′−H4		1.097	1.092
	C2′−H5		1.097	1.094
	C1−Cu−C2[e]		179.7	180.4
	H4−Cu−C1		83.7	72.9
$[Me_2Cu\cdots(H-CH_2)_2O]^-$, **4**	C1−Cu, C2−Cu	1.973	1.969	1.981
	Cu−H1, Cu−H4	2.914	2.904	3.109
	C1−H1, C2−H4	2.830 (3.216)	2.817 (3.307)	2.984
	C1′−H1, C2′−H4	1.100	1.100	1.094
	C1′−H2, C2′−H5	1.105	1.105	1.098
	C1′−H3, C2′−H6	1.096	1.096	1.089
	C1−Cu−C2[e]	182.4	182.4	180.2
	H4−Cu−C1	67.6	67.5	67.6

[a] B3LYP/I data from ref 20a. [b] X-ray data from ref 35a. [c] X-ray data from ref 35b. [d] MP2 data from ref 47. [e] These values represent directional C1−Cu−C2 bond angles calculated according to φ(C1CuC2) = φ(C1CuH*i*) + φ(C2CuH*i*); values slightly exceeding 180° demonstrate that the copper apex of DMCA is directed toward H*i*. There, the fact is used that in **2**, **3**, and **4**, the atoms Cu, C1, C2 and the hydrogen atoms of the C−H*i* bonds directly interacting with DMCA (**2**: H*i* = H1; **3**: H*i* = H4; **4**: H*i* = H1 or H4) lie practically in the same plane.

Table 2. Internuclear Distances (Å), Bond Path Lengths (Å) in Parentheses, and Bond Angles (φ, deg) for B3LYP/III- and MP2-Optimized Dimethylcuprate(I) Anion and Its Complex with Methane

molecule	parameter	B3LYP/III	MP2/II	MP2/III
$(Me_2Cu)^-$, **1**	Cu−C1, Cu−C2	1.966	1.943, 1.935,[a] 1.929,[b] 1.937,[b] 1.963[c]	1.904
	C1−H, C2−H	1.100	1.100	1.098
	C1−Cu−C2[d]	180.0	180.0	180.0
$(Me_2Cu\cdots H-CH_3)^-$, **2**	C1−Cu	1.966	1.945	1.905
	C2−Cu	1.965	1.943	1.903
	Cu−H1	3.222 (3.271)	2.865	3.086
	C1−H1	3.226	2.817 (3.170)	2.824 (2.915)
	C1′−H1	1.089	1.089	1.085
	C1′−H2	1.089	1.089	1.085
	C1′−H3, C1′−H4	1.089	1.089	1.086
	C1−Cu−C2[d]	180.2	180.4	180.0
	H1−Cu−C1	72.3	68.7	63.9

[a] X-ray data from ref 35a. [b] X-ray data from ref 35b. [c] MP2 data from ref 47. [d] See footnote *e* in Table 2.

result, to the shift of the methane molecule toward the C1-methyl group. The values of the H1−Cu−C1 angle (Tables 1 and 2, Figure 1) clearly confirm this trend and show that MP2 calculations overestimate the interaction of methane with the C1-methyl group compared with B3LYP calculations. As in the case of **1**, MP2/III results in too short Cu−C bonds of 1.903 and 1.905 Å in complex **2** (Table 2) compared with those in experimentally studied SSIPs of DMCA (1.929−1.937 Å),[35] MP2/II-calculated *d*(Cu−C) values of 1.943 and 1.945 Å being again much closer to experimental data.[35] Thus the relativistic MP2/III calculations strongly overestimate Cu−C interactions in **1** and **2**. It could not be excluded therefore that the interaction of methane with the C1-methyl group of DMCA is also overestimated, and this overestimation leads to a larger stability of **2** compared with that predicted by other methods used.

The main goal of this work is to evaluate the possibility that DMCA and other diorganocuprate(I) anions can form complexes with C−H bonds of neutral ligands surrounding a countercation in diorganocuprates(I). To elucidate the nature of interactions involved in the formation of the complexes is the second goal of this work. The simplest possible complexes of DMCA with methane, propane, and DME were chosen as model systems. In relation to the goals stated, the MP2 calculations, which can overestimate the stability of the target complexes, are obviously less suitable, as a complex with an overestimated computed stability is not guaranteed to exist in reality. Therefore, B3LYP calculations resulting in slightly underestimated stabilities of the investigated complexes were preferred. The B3LYP approach is also legitimized by the fact that, despite the differences mentioned above for bond lengths and H1−Cu−C1 angles, B3LYP and quite demanding MP2 calculations result in similar structures of **2** as well as similar interactions within **2** (see below). Therefore, sufficiently larger complexes of DMCA with propane and DME were studied using the less demanding B3LYP calculations. B3LYP/II-optimized geometries and data on QTAIM and NBO analysis of B3LYP/II wave functions for all complexes studied will be mainly discussed unless otherwise mentioned.

Table 3. Dissociation Energies ($E°$, kcal/mol), BSSEs (E_{BSSE}, kcal/mol), and BSSE-Corrected Dissociation Energies (E^{CP}, kcal/mol) for Dimethylcuprate(I) Anion Complexes with Methane, Propane, and DME

complex	method	$E°$	E_{BSSE}	E^{CP}
$(Me_2Cu\cdots H-CH_3)^-$, **2**	B3LYP/I//B3LYP/I	0.81	−0.88	−0.07
	B3LYP/II//B3LYP/II	0.93	−1.05	−0.12
	B3LYP/XL//B3LYP/II	0.22	−0.12	0.10
	B3LYP/III//B3LYP/III	0.45	−0.02	0.43
	B3LYP/IV//B3LYP/III	0.44	−0.03	0.41
	B3LYP/XL//B3LYP/XL	0.49	−0.10	0.39
	MP2/II//MP2/II	0.86	−1.98	−1.12
	MP2/XL//MP2/II	1.59	−0.48	1.11
	MP2/III//MP2/III	1.38	−0.33	1.05
	MP2/IV//MP2/III	1.41	−0.33	1.08
$(Me_2Cu\cdots MeCH_2Me)^-$, **3**	B3LYP/II//B3LYP/II	1.25	−0.78	0.47
	B3LYP/XL//B3LYP/II	1.03	−0.13	0.90
	B3LYP/XL//B3LYP/XL	1.33	−0.15	1.18
$[Me_2Cu\cdots(H-CH_2)_2O]^-$, **4**	B3LYP/I//B3LYP/I	3.11	−0.45	2.66
	B3LYP/XL/B3LYP/I	2.96	0.01	2.97
	B3LYP/II//B3LYP/II	2.24	−0.10	2.14
	B3LYP/XL//B3LYP/II	2.87	−0.05	2.82
	B3LYP/XL//B3LYP/XL	3.15	−0.10	3.05

B3LYP optimizations of complexes of DMCA with propane and DME without any constraints led to the complexes **3** and **4** as real minima on the corresponding PESs. The 3D structures of **3** and **4** as defined by the molecular graphs are presented in Figure 1. The dissociation energies of **3** and **4** into the isolated **1** and the corresponding neutral ligand are listed in Table 3. The E^{CP} values show that **3** and **4**, according to B3LYP/II//B3LYP/II, B3LYP/XL//B3LYP/II, and B3LYP/XL//B3LYP/XL theory levels, are stable with respect to the separated reactants. Even B3LYP/I//B3LYP/I-calculated **4** with the E^{CP} of 2.7 kcal/mol is stable. Despite appreciably larger separations between DMCA and propane in **3** as well as between DMCA and DME in **4**, predicted by B3LYP/XL optimization, this theory level yields the largest E^{CP} of 1.2 and 3.0 kcal/mol for **3** and **4**, respectively. The binding energies of hydrogen-bonded complexes have been shown to correlate with the acidity of the C−H proton donors.[37a] Therefore, a larger stability of **3** and **4** compared to **2** is most likely explained by their higher binding energies due to a lower intrinsic energy of the C(2)−H bonds in propane and the C−H bonds in DME than in methane.[42] One can conclude that coordination of C−H bonds of ethereal solvents and crown ethers to diorganocuprate(I) anions is feasible. However, the largest stabilities of **3** and **4**, calculated using the B3LYP/XL method, are significantly smaller than those previously calculated for complexes of Cu^+ with C−H bonds of neutral ligands.[9a,b,43] A lower positive charge on the copper (see below), strong Pauli repulsion between the closed shells of the neutral ligands studied, and the negatively charged DMCA are obviously responsible for the much lower binding energies of complexes studied and for about 1 Å larger internuclear Cu···H distances (d(Cu···H)) in **2**, **3**, and **4** (Tables 1 and 2) than in Cu^+ complexes.[9b]

According to QTAIM,[15,44] a molecular structure is defined as a network of interatomic interaction lines linking nuclei. This network is called a molecular graph. A (3,−1) critical point (CP) between two linked atoms should also exist. The presence of a (3,−1) CP and the associated bond path revealed by the topological analysis for a stable equilibrium structure are "both necessary and sufficient for two atoms to be bonded to one another in the usual chemical sense of the word".[44] For a stable equilibrium structure, the (3,−1) CP and the associated atomic interaction line are termed the bond CP (BCP) and bond path (BP), respectively. Selected internuclear distances, bond path lengths, and bond angles for the complexes studied are listed in Tables 1 and 2. The electron density[15] (ρ_{BCP}), the Laplacian[15] ($\nabla^2\rho_{BCP}$), the local energy density[45] (H_{BCP}), and the ellipticity[15,45a,46] (ϵ) values for the most important BCPs of **1**−**4** are presented in Table S1 of the Supporting Information. For **1** the QTAIM analysis of B3LYP and MP2 wave functions shows that in a vacuum the Cu−C bond is strongly polarized toward the carbon atom and is appreciably ionic, as evidenced by a low H_{BCP} value for the Cu−C bond (Table S1). This agrees with the calculations previously published,[47] which were based on MP2 wave functions. The residual partially covalent character was also proven experimentally in solution through the NMR detection of $^2J_{CC}$ and $^3J_{HC}$ scalar couplings across Cu.[48] According to the calculations, a strong polarization of **1** results in a positive QTAIM and NBO charge at Cu (q_{Cu}) (Table S2). Remarkably, the QTAIM charge at Cu calculated using both B3LYP and MP2 densities decreases, whereas the NBO charge calculated using the same densities increases on the expansion of the basis set. For the carbon atoms of **1**, the NBO analysis of B3LYP and MP2 densities predicts a too high negative charge (about −1.2), while for the hydrogens a positive NBO charge (0.14−0.18) was calculated. The negative charges at both carbon (from −0.28 to −0.38) and hydrogen (about −0.11) atoms predicted by QTAIM analysis seem to agree better with the appreciably ionic character of the Cu−C bond in **1** and with the hydridic nature of hydrogen atoms in DMCA.

In **2**, **3**, and **4** slightly larger positive charges at copper, as compared to **1** (Table S2), suggest that copper donates to methane, propane, or DME a larger electron charge than it accepts from these neutral ligands. This is confirmed by the calculation of changes in the electron populations (ΔN_i) using the equation $\Delta N_i = N_i^C - N_i^R$, with N_i^C and N_i^R being the electron populations of ith atom in the complex C and in the

(42) Dem′yanov, P. I.; Polestchuk, P. M.; Petrosyan, V. S., to be published.

(43) (a) Hill, Y. D.; Freiser, B. S.; Bauschlicher, C. W., Jr. *J. Am. Chem. Soc.* **1991**, *113*, 1507−1510. (b) Berthier, G.; Cimiraglia, R.; Daoudi, A.; Mestdagh, H.; Rolando, C.; Suard, M. *J. Mol. Struct. (THEOCHEM)* **1992**, *254*, 43−49.

(44) Bader, R. F. W. *J. Phys. Chem. A* **1998**, *102*, 7314−7323.

(45) (a) Cremer, D.; Kraka, E. *Angew. Chem.* **1984**, *96*, 612−614; *Angew. Chem., Int. Ed. Engl.* **1984**, *23*, 627−628. (b) Cremer, D.; Kraka, E. *Croat. Chem. Acta* **1984**, *57*, 1259−1281.

(46) Bader, R. F. W.; Slee, T. S.; Cremer, D.; Kraka, E. *J. Am. Chem. Soc.* **1983**, *105*, 5061−5068.

(47) Böhme, M.; Frenking, G.; Reetz, M. T. *Organometallics* **1994**, *13*, 4237−4245.

(48) Mobley, T. A.; Müller, F.; Berger, S. *J. Am. Chem. Soc.* **1998**, *120*, 1333−1334.

isolated reactant R, respectively. Although the QTAIM and NBO approaches predict quite different absolute charges at carbon and hydrogen atoms of **1**, **2**, **3**, and **4**, the ΔN_i values obtained by either of the methods agree much better (Tables S3 and S4) and show that electron charge is transferred not only from Cu but also from hydrogen and carbon atoms of DMCA. The charge transfer from DMCA to ligands results in an appreciable decrease of electron density on hydrogen and carbon atoms of hydrogen-bond-donating C−H bonds of methane, propane, or DME. The decrease of electron density on the hydrogen atom of the hydrogen-bond-donating C−H bond seems to be a general feature predicted for any hydrogen bonds.[37a] On the other hand, electron density is increased on hydrogen atoms of C−H bonds that do not interact directly with DMCA. Also, the QTAIM analysis of B3LYP/IV and MP2/IV densities for **2** and B3LYP/II density for **4** predicts an appreciable increase of electron density on the carbon atoms of methane and DME. This particularity is also a common feature of the hydrogen bond.[37a] Due to the donation of electron density from DMCA toward the interacting C−H bonds, a larger value of the density is obviously pushed away from the contacting H atoms to the corresponding carbons and then to the peripheral hydrogens. The Pauli repulsion between DMCA and closed shells of the ligands can also push electron density away from the contacting H atoms. Thus, changes of electron densities on different atoms of the target complexes do not allow describing unambiguously the origin of stabilizing interactions in these complexes. The second-order perturbation NBO analyses of electron densities calculated for the complexes give clearer insight into the nature of those interactions.[49]

B3LYP/II-calculated total second-order perturbation NBO stabilization energies (E_{st}(DMCA→L)) due to donations from DMCA to ligand L (L = methane, propane, DME) (3.2, 4.8, and 5.8 kcal/mol, respectively) are about 10 times larger than those (E_{st}(L→DMCA) for the reverse direction (Table S5). E_{st}-(DMCA→L) of 1.2 kcal/mol calculated for **2** using B3LYP/IV densities exceeds E_{st}(L→DMCA) by about 4 times. Much smaller E_{st}(L→DMCA) values are probably caused by the negative charge of DMCA that hampers the electron charge transfer toward the anion. Additionally, the second-order perturbation NBO analysis of B3LYP/II (Table S5) and B3LYP/IV (Table S6) densities shows that donation of electron charge from the copper center is one of the most important factors in the stabilization of these complexes. Thus in **2**, 46% (B3LYP/IV) or even 51% (B3LYP/II) of the E_{st}(DMCA→L) is related to the energy (E_{st}(LP(Cu)→L)) characterizing back-donations from lone pair (LP) orbitals of Cu to the σ^*(C1′−H1) and Rydberg (RY*) orbital of H1 of methane. In **3**, 46% of E_{st}-(DMCA→L) corresponds to the stabilization due to back-donations from Cu LPs to σ^*(C2′−H4) and RY*(H4) orbitals of propane. In **4**, back-donations from Cu to σ^*(C−H) and RY*-(H) orbitals of the C1′−H1 and C2′−H4 bonds of DME contribute only 29% to E_{st}(DMCA→L). LP(Cu) → L back-donations in **2**, **3**, and **4** are equivalent to the formation of Cu···H−C HBs. The $\nabla^2\rho_{BCP}$ values for BCPs describing Cu···H interactions in **2** and **3** (Table S1) are in the range 0.0093−0.139 au determined for HBs,[50] and the positive and small values of the H_{BCP} for the respective BCPs in **2** and **3** agree with H_{BCP} values characterizing closed-shell interactions including HBs.[15,44,45b,50c,51] The total NBO stabilization energy E_{st}-(TBD→CH) characterizing all back-donations to orbitals of one C−H bond linearly decreases from **3** to **2** to **4** (2.2, 1.6, and 0.8 kcal/mol) and correlates with the enlargement of d(Cu···H), E_{st}(TBD→CH) being 21, 25, and 11 times larger than the corresponding specific stabilization energies (E_{st}(CH→Cu)) due to donations from σ(C−H) orbitals to RY*(Cu) orbitals. On the contrary, for the complex of copper(I) cation (Cu^+) with one hydrogen of each of the terminal methyl groups of propane in the gas phase, the stabilization energy of the complex due to σ(C−H) → Cu donations (E_{st}(CH→Cu)) exceeds that due to Cu → σ^*(C−H) back-donations (E_{st}(BD→CH)) by 3 times.[9b] The E_{st}(XH→Cu)/E_{st}(BD→XH) ratio for interactions of Cu^+ with X−H bonds of $MeCH_2-XH_3$ (X = Si, Ge),[9b] HC≡C−XH_3, MeC≡C−XH_3, and HC≡C−XH_2Me (X = Si, Ge),[9a] and XH_3 (X = B, Al, Ga)[9c] was calculated to be between 3.0 and 4.0. Similar ratios of E_{st}(XH→Cu) and E_{st}(BD→XH) were found for complexes of Ni^+ with X−H bonds of $MeCH_2-XH_3$ (X = C, Si, Ge),[52a] H_2C=CH−XH_3 (X = C),[52a] and HC≡C−XH_3,[52b] whereas E_{st}(XH→Cu)/E_{st}(BD→XH) of 8.3 and 7.4 were found[52a] for complexes of Ni^+ with H_2C=CH−SiH_3 and H_2C=CH−GeH_3 (X = Si and Ge, respectively) in the gas phase. The interactions of Cu^+ and Ni^+ with X−H bonds, which are stabilized to a significantly larger extent through accepting electron charge from these bonds by metal cations, are considered[9,52] to be agostic interactions in accordance with the definition given for such interactions.[3] Using the energy criterion for complexes of DMCA, which are characterized by much larger E_{st}(TBD→CH) energies compared with E_{st}(CH→Cu) ones, allows us to conclude that interactions of C−H bonds of methane, propane, and DME with the Cu center of DMCA are hydrogen bonding, but not agostic interactions.

The presented data show that compared to complexes of Cu^+ the reduced positive charge at Cu in DMCA causes a drastic change in the interaction mode between Cu and the C−H bonds. The copper center of DMCA mainly donates electron density to the C−H bonds and forms Cu···H−C HBs, while Cu^+ mainly accepts electron density from these and other bonds; that is, it prefers agostic interactions with ligands.[9] The analysis of data obtained shows that the formation of **2**, **3**, and **4** is accounted for not only by Cu···H−C HBs but rather by multiple interactions differing in energy and leading to different E^{CP} values (Table 3). Therefore, there is, for example, no correlation between d(Cu···H) and E^{CP}.

For all structures calculated in this study as well as for **1** calculated at the Hartree−Fock level,[47] the NBO theory describes DMCA as a complex between a $Me(1)^-$ anion and a neutral Me(2)Cu(I). As a consequence of this computational artifact, only the donations from σ^*(Cu−C2) and σ(Cu−C2) into orbitals of the interacting C−H bonds are found. The fully symmetric structure of **4** (Figure 1) excludes the artificially calculated asymmetry, but proposes the interaction of both Cu−

(49) The second-order perturbation NBO analysis of MP2/II and MP/IV densities failed, as a bond orbital with an occupancy of −0.004 and −0.001 electron, respectively, was found in each of these cases.

(50) (a) Carroll, M. T.; Bader, R. F. W. *Mol. Phys.* **1988**, *65*, 695−722. (b) Koch, U.; Popelier, P. L. A. *J. Phys. Chem.* **1995**, *99*, 9747−9754. (c) Matta, C. F.; Hernández-Trujillo, J.; Tang, T.-H.; Bader, R. F. W. *Chem. Eur. J.* **2003**, *9*, 1940−1951. (d) Jensen, S. J. K.; Tang, T.-H.; Csizmadia, I. G. *J. Phys. Chem. A* **2003**, *107*, 8975−8979. (e) Wojtulewski, S.; Grabowski, S. J. *Chem. Phys. Lett.* **2003**, *378*, 388−394. (f) Sosa, G. L.; Peruchena, N. M.; Contreras, R. H.; Castro, E. A. *J. Mol. Struct. (THEOCHEM)* **2002**, *577*, 219−228. (g) Rybarczyk-Pirek, A. J.; Grabowski, S. J.; Malecka, M.; Nawrot-Modranka, J. *J. Phys. Chem. A* **2002**, *106*, 11956−11962. (h) Grabowski, S. J.; Sokalski, W. A.; Leszczynsky, J. *J. Phys. Chem. A* **2004**, *108*, 5823−5830.

(51) (a) Bader, R. F. W.; Essén, H. *J. Chem. Phys.* **1984**, *80*, 1943−1960. (b) Bone, R. G. A.; Bader, R. F. W. *J. Phys. Chem.* **1996**, *100*, 10892−10911. (c) Hernández-Trujillo, J.; Bader, R. F. W. *J. Phys. Chem. A* **2000**, *104*, 1779−1794.

(52) (a) Corral, I.; Mó, O.; Yáñez, M. *New J. Chem.* **2003**, *27*, 1657−1664. (b) Corral, I.; Mó, O.; Yáñez, M. *Theor. Chem. Acc.* **2004**, *112*, 298−304.

C1 and Cu−C2 bond orbitals with the C−H bonds. The same should be valid for **2** and **3**. Despite the limitations described, the NBO theory gives an interesting insight into the nature of interactions in the complexes studied.

According to the NBO analysis, **1** and DMCA in **2**−**4** are formed mainly due to a LP(C1)→σ*(Cu−C2) donor−acceptor interaction. A strong interaction of the LP(C1) of the methyl anion with the σ*(Cu−C2) orbital of Me(2)Cu results in a high occupancy of σ*(Cu−C2) in **1** (0.33, B3LYP/II; 0.29 au, B3LYP/IV), **2** (0.32, B3LYP/II; 0.29 au, B3LYP/IV), **3** (0.32 au), and **4** (0.32 au). Sufficiently small (0.28−0.37 au) energy gaps (ΔE_{AD}) separating σ*(Cu−C2) and σ*(C−H) orbitals of methane, propane, and DME lead to appreciable stabilization of σ*(Cu−C2) → σ*(C−H) interactions (Tables S5 and S6). The respective σ*(Cu−C2) orbitals consist of more than 80% of copper atomic orbitals, and hence the positively charged copper center is mainly accounted for by these interactions. The contribution of the σ*(Cu−C2) → σ*(C−H) interactions into E_{st}(DMCA→L) of **2**, **3**, and **4** was found to be 37, 32, and 21%. Another important feature of B3LYP/II-calculated complexes of DMCA is the donation from the σ(Cu−C2) orbital to the corresponding σ*(C−H) orbitals of the ligands. In all the complexes studied the σ(Cu−C2) and σ*(C−H) orbitals are separated by a significantly larger gap ΔE_{AD} of 0.80 au because the bonding σ(Cu−C2) orbital lies significantly lower than σ*(Cu−C2). Consequently, this leads to a sufficiently lower E_{st} for σ(Cu−C2) → σ*(C−H) interactions for **2**, **3**, and **4**. In place of σ(Cu−C2) → σ*(C−H) interactions NBO analysis of B3LYP/IV density reveals σ*(Cu−C2) → RY*(H1) donations. The described donations from σ*(Cu−C2) and σ(Cu−C2) are second-order Cu−C→H−C and Cu−C→H orbital interactions, which obviously cannot be considered either as hydrogen bonding or as agostic interactions. Their contributions to the total E_{st}(DMCA→L) of **2**, **3**, and **4** (45, 43, and 38%, respectively) are comparable with those of the respective back-donations from copper LPs to σ*(C−H) and RY*(H) orbitals discussed above.

In addition to the described two main types of interactions, a number of significantly weaker second-order charge transfers contribute to the formation of **2**, **3**, and **4** according to NBO and MO analyses. Thus, MO analysis of **2** shows, for example, that methane interacts additionally with the C1-methyl group via deep MOs (Figures 2), which is confirmed by the NBO analysis (Table S5), and leads most probably to the tilt of the methane molecule toward the C1-methyl group (Figures 1 and 2). QTAIM analysis does not deal with orbitals, but describes interactions between atoms A and B as a local pairing of the densities of opposite spin electrons, i.e., the exchange of electrons between the basins of these atoms.[15,44,53a,b] The exchange of electrons and their accumulation between nuclei of atoms A and B balances the force of repulsion on the nuclei and lowers the potential energy of the nuclei. The pairing of electrons depending on the distance between A and B and the strength of the interaction should be distinguished from the Lewis concept requiring one pair of electrons per bond between two atoms. The delocalization index (δ(A,B)) is a measure of the number of electrons between atoms A and B and the extent of the sharing of electrons between atomic basins of any given pair of atoms.[53]

(53) (a) Fradera, X.; Austen, M. A.; Bader, R. F. W. *J. Phys. Chem. A* **1999**, *103*, 304−314. (b) Cortés-Guzmán, F.; Bader, R. F. W. *Coord. Chem. Rev.* **2005**, *249*, 633−662. (c) Bader, R. F. W.; Matta, C. F.; Cortés-Guzmán, F. *Organometallics* **2004**, *23*, 6253−6263. (d) Merino, G.; Vela, A.; Heine, T. *Chem. Rev.* **2005**, *105*, 3812−3841. (e) Poater, J.; Duran, M.; Solà, M.; Silvi, B. *Chem. Rev.* **2005**, *105*, 3911−3947.

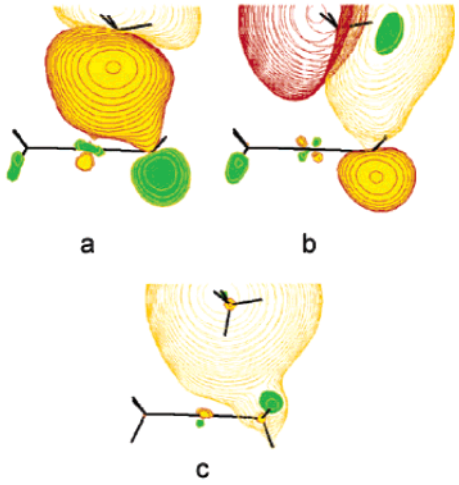

Figure 2. Contour maps of some MOs for the B3LYP/II-calculated DMCA−methane complex. The MO energies (E) are given in atomic units [au]: HOMO−11, $E = -0.255$, contour value 0.004 (a); HOMO−12, $E = -0.265$, contour value 0.001 (b); HOMO−16, $E = -0.563$, contour value 0.001 (c).

Two types of interactions are distinguished by QTAIM:[15,44,50c,51] the shared interactions and the closed-shell interactions. An accumulation of electron density between the nuclei along a BP is the main factor in the potential energy lowering in the case of shared interactions, and therefore the energy density H_{BCP} is negative in this case. For shared nonpolar interactions $\nabla^2\rho_{BCP} < 0$ as a result of a predominating perpendicular contraction of the density toward the BP, while for a polar interaction, $\nabla^2\rho_{BCP}$ can be positive or negative, but large in magnitude.[53a] Relatively large positive $\nabla^2\rho_{BCP}$ and small but negative H_{BCP} values are observed for C−Cu bonds in **1** and complexes **2**−**4** (Table S1). The minimization of the energy of an interaction between two atoms leads to the appearance of an atomic interaction line (a bond path in the case of a stable equilibrium structure): a line between two atoms along which the potential energy of electron density is maximally negative with respect to any neighboring line.[15,44] For a molecule in its stable state the presence of a (3,−1) BCP between a pair of atoms and its associated BP is, as was mentioned above, both necessary and sufficient for the two atoms to be bonded to one another. A BCP is a point where $\nabla\rho(\mathbf{r}) = 0$ and where the density attains its minimal magnitude along the BP. Since the electron density is concentrated between atoms bonded via shared interactions, the ρ_{BCP} value at BCP is relatively large (>0.1 au as a rule).[15,44,51c,53a] Values of ρ_{BCP} calculated for C−Cu bonds in **1** and complexes **2**−**4** only slightly exceed 0.1 au.

In the case of closed-shell interactions, dipolar and quadrupolar polarizations of approaching closed-shell atoms or ions remove electron density from the area of overlap and facilitate the approach of two atoms (ions) and the interpenetration of their densities, the penetration being limited to create a value of ρ_{BCP} that is approximately equal to the sum of densities of the unperturbed atoms.[51c] Thus, in the case of a closed-shell interaction the electron density is not shared between but concentrated within the atomic basins, leading to a weak interaction. Despite the lack of a significant accumulation of density between interacting atoms, a BCP exists between these atoms. Closed-shell interactions are dominated by the kinetic energy, and therefore the energy density H_{BCP} and $\nabla^2\rho_{BCP}$ are positive. Positive and very small H_{BCP} and $\nabla^2\rho_{BCP}$ values are observed for Cu···H contacts in **2** and **3**, both C···H contacts

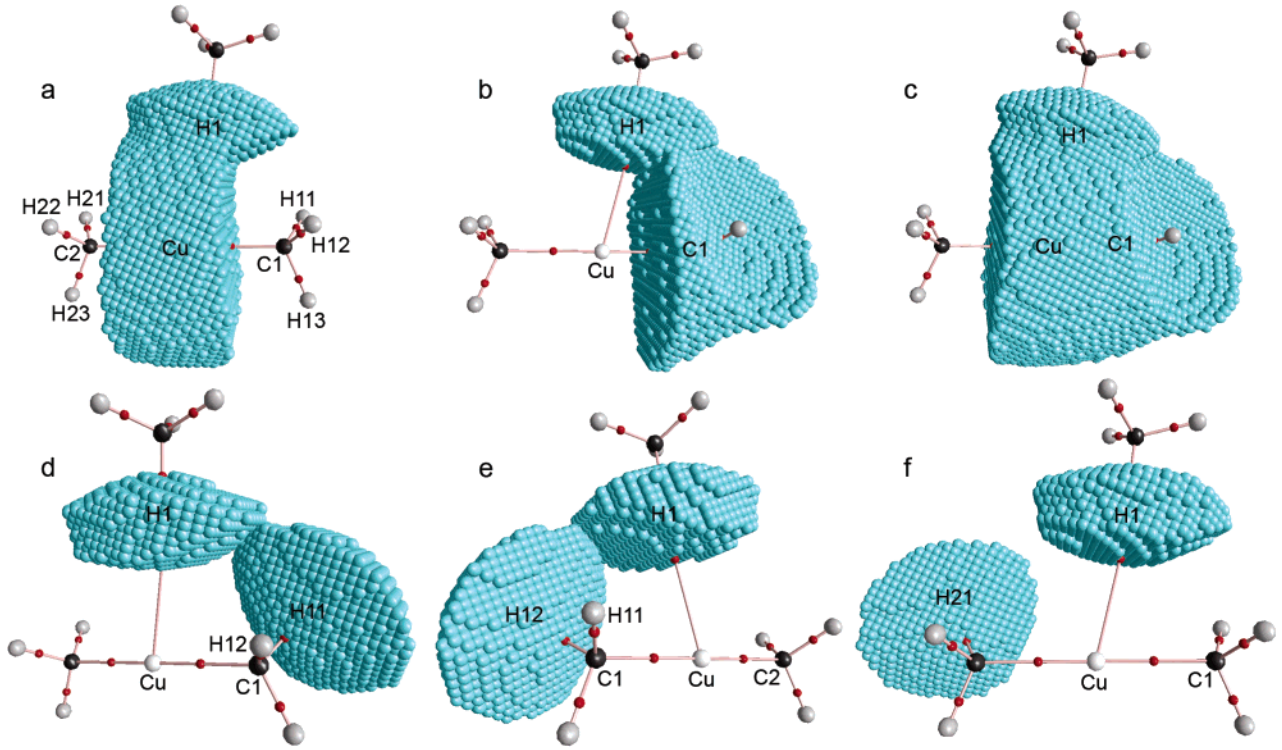

Figure 3. Molecular graph for the DMCA−methane complex **2a** and envelopes for some atomic basins bound by surfaces of $\rho = 0.001$ au. Black and gray spheres represent carbon and hydrogen atoms, respectively. Small red spheres are bond critical points.

in **4**, and the H···H contact in **3** (Table S1). Worthy of note is that B3LYP/II//B3LYP/II- and even B3LYP/I//B3LYP/I-calculated values of ρ_{BCP}, H_{BCP}, and $\nabla^2\rho_{BCP}$ for the Cu···H contact in **2** are very similar to those computed for the similar contact in **2c** using the correlated MP2/II//MP2/II method. Thus, all three methods estimate quite similarly the strength of the weak Cu···H interaction, despite that MP2 predicts appreciably stronger C−Cu interactions: (i) for these bonds the MP2/II//MP2/II-calculated ρ_{BCP} and positive $\nabla^2\rho_{BCP}$ values are somewhat larger and the H_{BCP} values are more negative compared to those computed using B3LYP/I//B3LYP/I and B3LYP/II//B3LYP/II method; (ii) C−Cu bonds in MP2/II-optimized **2c** are shorter than in B3LYP/II-optimized **2a**. It is interesting that MP2/IV//MP2/III-computed ρ_{BCP}, H_{BCP}, and $\nabla^2\rho_{BCP}$ values for the C1···H1 contact in **2d** are comparable with those computed for the Cu···H contacts in **2a** and **2c**. On the contrary, B3LYP/IV//B3LYP/III-calculated ρ_{BCP}, H_{BCP}, and $\nabla\ ^2\rho_{BCP}$ values for the Cu···H interaction in **2b** are twice as low, obviously because in this complex d(Cu···H1) of 3.222 Å is much larger than in **2a** (2.850 Å).

In contrast to the computation of properties of BCPs, delocalization indices can be also computed for a pair of atoms that are not linked by BP. Delocalization indices δ(A,B) for different pairs of atoms of complexes **2**−**4** (Table S7) were computed using B3LYP densities.[54] First of all it is worth mentioning that a high degree of delocalization of electrons between carbon and copper atoms of **1** (δ(C,Cu) = 0.823, B3LYP/II; 0.835, B3LYP/IV) and in DMCA of complexes **2**−**4** (Table S7) demonstrates a significantly large sharing of the bonded C−Cu pairs and confirms NMR data on a substantial covalent character of the C−Cu bonds in DMCA.[48] Somewhat smaller δ(C,Cu) as well as δ(C1,Hi) (i = 11, 12, 13) and δ-(C2,Hj) (j = 21, 22, 23) computed for **2**−**4**, compared to those found for **1** (δ(C1,Hi) = δ(C2,Hj) = 1.009, B3LYP/II; 1.019, B3LYP/IV), additionally confirm charge transfer from DMCA to the neutral ligands. On the other hand, distinctly smaller δ-(C1,Hi) (i = 11, 12, 13) indices compared to δ(C2,Hj) (j = 21, 22, 23) ones predicted for **2** and **3** confirm second-order donor−acceptor stabilizing interactions (bondings) of C−H bonds of methane and propane with the C(1)-methyl but not with the C(2)-methyl group of DMCA in **2** and **3**. However, according to QTAIM, two atoms are bonded if they share an interatomic surface and are consequently linked by a bond path,[15,44,51c,53a,55] the latter being considered as a universal indicator of bonded interactions.[44]

The analysis of the envelopes of atomic basins for **2a**, **2b**, and **2c** shows that in addition to the interatomic surface S(Cu,-H1) between Cu and H1 (Figure 3a) linked by BP_{H1Cu} (Figure 1) small but clearly pronounced interatomic surfaces S(H1,-C1), S(H1,H11), and S(H1,H12) between H1 and the atoms of the C(1)-methyl group exist (Figures 3b, 3d, and 3e, respectively), but not between H1 and the atoms of the C(2)-methyl group (Figure 3f). The molecular graph and the envelopes for some atomic basins are exemplified in Figure 3 for complex **2a** only. On the other hand, in MP2/IV//MP2III-calculated **2d**, in which DMCA and methane are linked by a single BP_{1-1} between H1 and C1 (Figure 1), the analysis of the envelopes reveals the existence of S(Cu,H1) (Figure 4a), S(H1,H11), and S(H1,H12) (not shown in Figure 4) in addition to S(H1,C1) (Figure 4b). Thus, in all **2** complexes H1 shares interatomic surfaces and consequently is bonded simultaneously with Cu, C1, H11, and H12. Even though QTAIM[15,44,51c,53a] considers only interactions between two atoms, an atom with a bond or one bond with another one, Figures 3 and 4, can be considered to confirm NBO predictions on interactions of the C1′−H1 bond of methane with Cu and C1 centers as well as with the Cu−C1 bond (see above). From the analysis of the envelopes for basins of key atoms of **2a**−**2d** one could thus expect the existence of four BCPs (denoted as primary BCPs) between H1 and Cu

(54) Strictly speaking, delocalization indices apply only to a molecule in which all molecular orbitals are doubly occupied. Therefore, the indices based on MP2 densities are not discussed here.

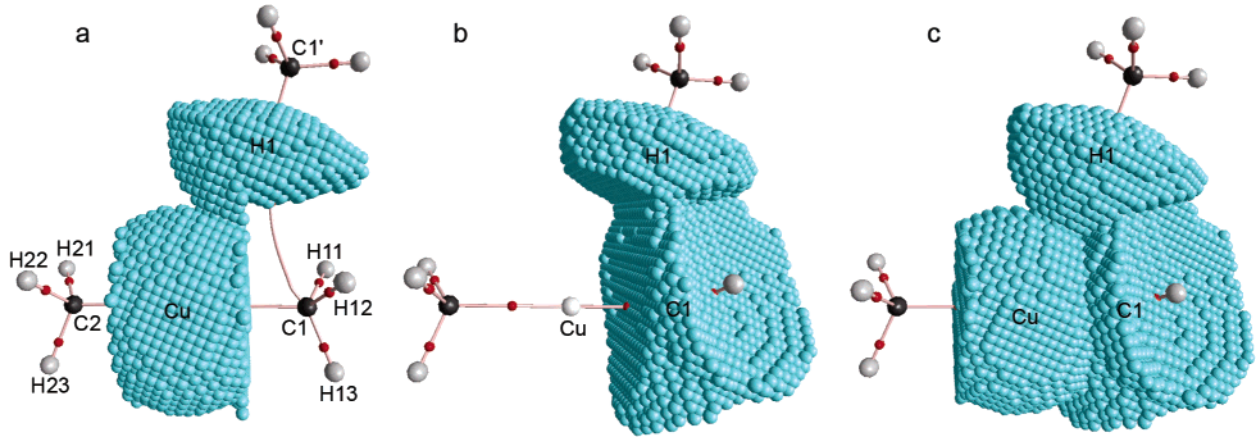

Figure 4. Molecular graph for the MP2/IV//MP2/III-computed DMCA−methane complex **2d** and envelopes for some atomic basins bound by surfaces of $\rho = 0.001$ au. Black and gray spheres represent carbon and hydrogen atoms, respectively. Small red spheres are bond critical points.

Scheme 1. Hypothetical Primary Bond and Ring Critical Points (small filled and empty circles, respectively) and Primary Bond Paths Linking the C1′−H1 Bond of Methane with the Cu Atom and Atoms of the C(1)-Methyl Group in the DMCA−Methane Complex, and Coalescences of These Critical Points into a Single Bond Critical Point between (a) H1 and Cu Atoms (BCP_{1-Cu}) or (b) H1 and C1 Atoms (BCP_{1-1}) and Its Associated Bond Path (BP_{1-Cu} or BP_{1-1}, respectively)

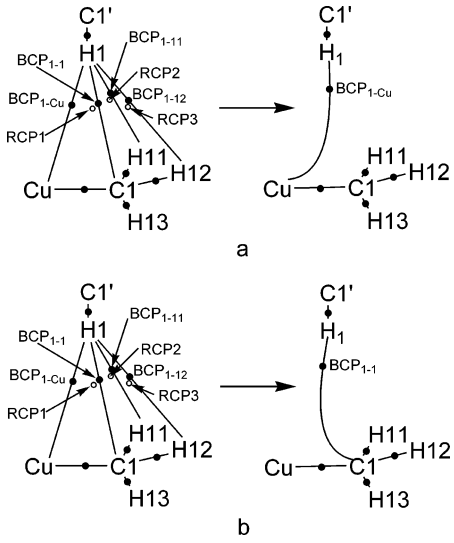

(BCP_{1-Cu}), H1 and C1 (BCP_{1-1}), H1 and H11 (BCP_{1-11}), and H1 and H12 (BCP_{1-12}) and their associated primary bond paths (BP_{1-Cu}, BP_{1-1}, BP_{1-11}, and BP_{1-12}, respectively) in molecular graphs for these complexes. These BCPs and BPs as well as the required three ring critical points (RCP1, RCP2, and RCP3) are exemplified for **2** in the left parts of Scheme 1. The closeness of atoms and critical points in the primary structure should result most likely in very similar properties of the primary bond and ring CPs, which can lead to a catastrophe.[26b,50c,d,51b,57] This catastrophe would induce the coalescence[15,50c,51b] of the primary bond and ring CPs[56] and result in the formation of a new topologically unstable BCP and its associated BP. The bond path is the line of maximum density between two atoms.[15,44,51c] The analysis of delocalization indices (Table S7) shows that in the space between DMCA and methane in **2a** and **2b** maximum density is between H1 and Cu. According to NBO data (see above), the strongest stabilizing donor−acceptor interaction is observed also between H1 and Cu, as well as between H1 and the Cu−C bonds. In the space between H1 and C1 the density is lower than that between H1 and Cu, but much higher than between H1 and H11, as well as H1 and H12. NBO data confirm a stronger interaction of H1 with C1 compared with that of H1 with C1−H11, C1−H12, and C1−H13 bonds. One must expect therefore that the bond path resulting from the coalescence of the primary critical points should link H1 just with the Cu atom and deviate slightly toward both C1 and the C1−Cu bond (Scheme 1a), which is observed in fact for **2a** and **2b** (Figure 1). Compared to **2a** and **2b**, with H1−Cu−C1 angles of 78.0° and 72.3°, methane in **2c** is shifted toward the C(1)-methyl group (H1−Cu−C1 angle is 68.7°), and consequently the interaction of C1′−H1 and H1 with the C(1)-methyl group (with C1 particularly) should increase. This increase, as well as the interaction of densities of C1′−H1 bond and H1 atom with the density of the C1−Cu bond, for which ρ_{BCP} is the largest in the row **2c** (0.110 au) > **2b** (0.109 au) > **2a** (0.105 au), result most likely in a dramatic deviation of the BP_{1-Cu} toward the C(1)-methyl group and BCP_{C1Cu} (Figure 1). In **2d** methane is even more tilted toward the C(1)-methyl group (H1−Cu−C1 angle is 63.7°), and both the C1′−H bond and H1 atom interact obviously stronger with this group (and particularly with C1 atom) than with the Cu atom. That interaction leads to the transformation of four primary BPs into the BP_{1-1} that links H1 and C1 (Scheme 1b). A small deviation of BP_{1-1} toward the Cu center and the C1−Cu bond in the molecular graph for **2d** (Figure 1) is most likely because a weak interaction of the C1′−H bond and H1 still exists with both the Cu atom and density of the C1−Cu bond. The ellipticity of 1.66 for BCP_{1-Cu} in **2c** is very high, demonstrating that this complex is topologically unstable. The length of the bond path linking Cu and H1 (l(Cu···H1)) in **2c** exceeds d(Cu···H1) by 0.3 Å, which provides additional evidence of the topological instability of this complex. Since a topologically unstable structure is not necessarily an energetically unstable one,[58] as in the case of **2c**, the latter complex is most probably topologically unstable with respect to the BP_{1-Cu}, which is a result of the catastrophe described above. In **2a** and **2b** the ellipticity of density at the bond critical

(55) Matta, C. F.; Castillo, N.; Boyd, R. J. *J. Phys. Chem. A* **2005**, *109*, 3669−3681.

(56) The coalescence of each pair of BCP and RCP does not breach the Poincaré−Hopf relationship.[16,55]

(57) (a) Cioslowski, J.; Mixon, S. T. *Can. J. Chem.* **1992**, *70*, 443−449. (b) Alkorta, I.; Elguero, J. *Chem. Phys. Lett.* **2003**, *381*, 505−511. (c) Bader, R. F. W.; Matta, C. F. *Inorg. Chem.* **2001**, *40*, 5603−5611.

(58) Ritchie, J. P.; Bachrach, S. M. *J. Am. Chem. Soc.* **1987**, *109*, 5909−5916.

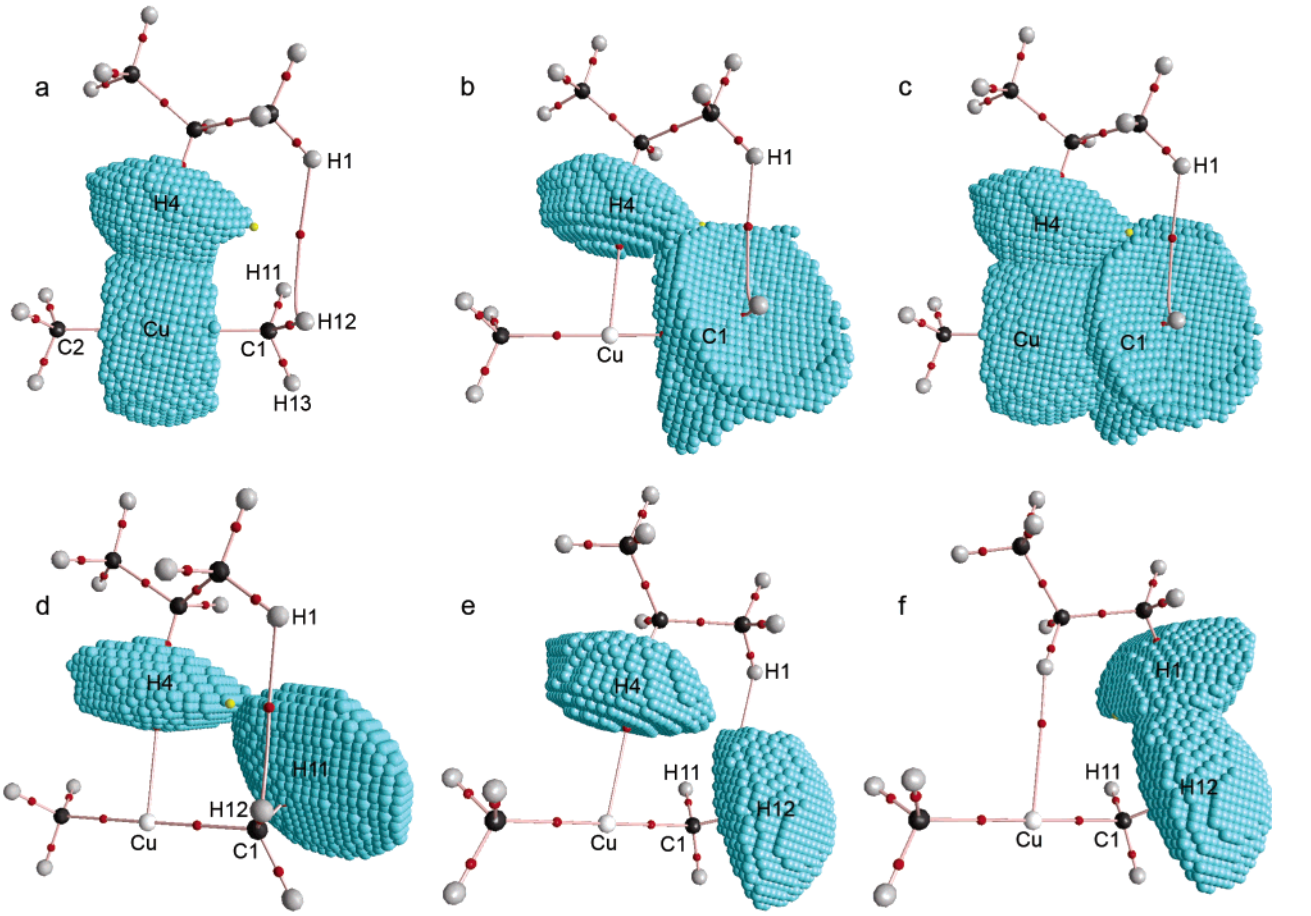

Figure 5. Molecular graph for the DMCA−propane complex **3** and envelopes for some atomic basins bound by surfaces of $\rho = 0.001$ au. Black and gray spheres represent carbon and hydrogen atoms, respectively. Small red and yellow spheres are bond and ring critical points, respectively.

point for the H1···Cu interaction and the differences between l(Cu···H1) and d(Cu···H1) are appreciably less than in **2c**, but significantly larger compared with those for the C−Cu bonds (Table S1) or C−H bonds in all the complexes studied. Hence, one can conclude that **2a** and **2b** are also topologically unstable with respect to the BP_{1-Cu}, because the last is the result of a coalescence of primary bond and ring critical points described above.

Compared to **2**, propane in **3** is slightly shifted toward Cu (Table 1), and consequently the interaction of the C2′−H4 bond and H4 with Cu should increase compared to **2a**, while the strength of interactions with the C(1)-methyl group of DMCA should decrease. A comparison of the values of ρ_{BCP}, H_{BCP}, and $\nabla^2\rho_{BCP}$ (Table S1) and δ(H4,Cu) and δ(H4,C1) (Table S7) as well as of the NBO stabilization energies for **3** and **2** confirms that conclusion. As in the case of **2**, an analysis of envelopes of atomic basins of **3** (Figure 5) reveals the complexity of the bond path for the Cu···H contact. That bond path obviously results from a coalescence of primary BCP_{4-Cu}, BCP_{4-1}, and BCP_{4-11}. Despite a delocalization index of 0.0008 computed for the pair of atoms H4 and H12, there is neither overlapping (Figure 5e) nor BCP between the basins of these atoms (Figures 1 and 5). In place of an H4···H12 interaction, a significant overlapping (Figure 5f) and BCP between H1 and H12 are observed (Figures 1 and 5). A slightly shorter Cu···H distance in **3** (Table 1) and larger E^{CP}value predicted for this complex (Table 3) compared to **2** can be explained by a stronger interaction of Cu with the more acidic C2′−H4 bond of propane[42] as well as by the additional H1···H12 interaction (Figures 1 and 5). The space requirement of the H1···H12 interaction decreases simultaneously the interaction between H4 and the C(1)-methyl group of DMCA and leads to a larger H4−Cu−C1 angle in **3** than in **2**. The H1···H12 hydrogen−hydrogen interaction in **3** corresponds to a donation from σ(C1−H12) of DMCA to σ^*(C1′−H1) of propane. For the H1 atom of propane in **3** both QTAIM and NBO predict a positive charge, whereas for H12 of DMCA QTAIM predicts a small negative charge (−0.11) and NBO a small positive charge (0.18). Experimental[4i,59] and theoretical[4i,50c,60,61] data show that stabilizing interactions between two hydrogen atoms bearing identical or similar charges may exist. However, the hypothesis of hydrogen−hydrogen interactions was seriously questioned recently.[62] A more probable explanation of the H1···H12 interaction in **3** is a distinctly pronounced hydridic property of H12 (as well as the rest of the hydrogen atoms of DMCA) as predicted by QTAIM, resulting in a contact with the positively charged H1. The formation of close contacts between hydridic H atoms and acidic C−H, N−H, or O−H bonds is a well-known phenomenon in chemistry,[2b,4g,i,50h,63a−k] and this type of interaction was referred to as a dihydrogen bond.[63k] Typical compounds, for which dihydrogen bonds were found and studied, are transition metal hydrides and hydrides of some main group elements.[2b,4d,f,g,i,50h,63a−d,j,l]

(59) Bombicz, P.; Czugler, M.; Tellgren, R.; Kálmán, A. *Angew. Chem.* **2003**, *115*, 2001−2004; *Angew. Chem. Int. Ed.* **2003**, *42*, 1957−1960.
(60) Novoa, J. J.; Whangbo, M.-H.; Williams, J. M. *J. Chem. Phys.* **1991**, *94*, 4835−4841.
(61) Bader, R. F. W. *Chem. Eur. J.* **2006**, *12*, 2896−2901.
(62) (a) Dunitz, J. D.; Gavezzotti, A. *Angew. Chem.* **2005**, *117*, 1796−1819; *Angew. Chem., Int. Ed.* **2005**, *44*, 1766−1787. (b) Poater, J.; Solà, M.; Bickelhaupt, F. M. *Chem. Eur. J.* **2006**, *12*, 2889−2895. (c) Poater, J.; Solà, M.; Bickelhaupt, F. M. *Chem. Eur. J.* **2006**, *12*, 2902−2905.

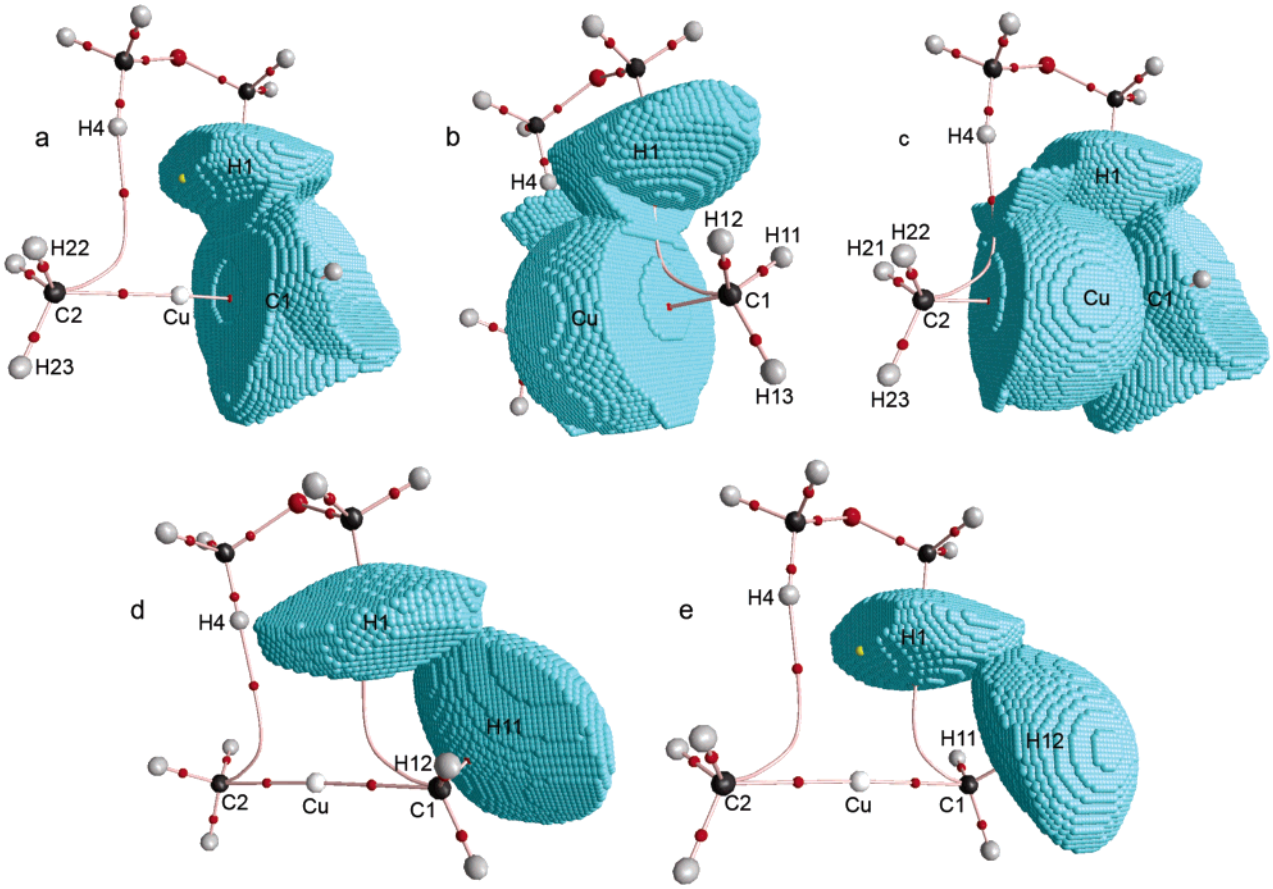

Figure 6. Molecular graph for the DMCA−dimethyl ether complex **4** and envelopes for some atomic basins bound by surfaces of ρ = 0.001 au. Black and gray spheres represent carbon and hydrogen atoms, respectively. Small red and yellow spheres are bond and ring critical points, respectively.

The formation of dihydrogen bonds with hydrogen atoms bound to carbanionic centers is less studied.[4a,i,63a,m−o] On the basis of the hydridic nature of the H12 atom predicted by QTAIM, the H1···H12 interaction in **3** can be considered a dihydrogen bond.

For **4**, only the interactions of H1 and H4 of DME with C1 and C2 of DMCA but not with Cu are predicted by QTAIM analysis (Figure 1), although the H1···Cu and H4···Cu separations are comparable with the H1···C1 and H4···C2 internuclear distances (Table 1). In addition, the corresponding bond paths (BP_{1-1} and BP_{4-2}) are strongly curved (Figure 1), and their length l is about 0.4 Å longer than d(H1···C1) and d(H4···C2) internuclear distances, exceeding even those $l-d$ values previously published.[50c,d] Additionally, large ellipticity[15,45b,46] values of about 1.6 were predicted for BCP_{1-1} and BCP_{4-2} (Figure 1), reflecting structural instabilities of these bond paths. The topological instability of the H1···C1 and H4···C2 interactions in **4** is apparently the result of a catastrophe similar to that described for **2**, and more complex interactions of the C1′−H1 and C2′−H4 bonds of DME with DMCA are most likely realized. The complexity of these interactions is confirmed by the analysis of envelopes of atomic basins of **4** (Figure 6), MO analysis (Figure 7), and NBO data. The NBO data show that the donations from C−H bond orbitals of the C(1) and C(2) methyl groups of DMCA to orbitals of the C1′−H1 and C2′−H4 bonds of DME additionally contribute to these interactions. Thus, the interaction of the C(1)-methyl group is described as donations from σ(C1−H13), σ(C1−H11), and σ(C1−H12) to σ^*(C1′−H1). The donation from the first orbital is mainly realized as interaction of C1 with the C1′−H1 bond of DME, whereas donations from σ(C1−H11) and σ(C1−H12) orbitals should be considered as interactions of the C1−H11 and C1−H12 bonds with the same C1′−H1 bond. The difference in strength of σ(C1−H13) → σ^*(C1′−H1), σ(C1−H11) → σ^*(C1′−H1), and σ(C1−H12) → σ^*(C1′−H1) interactions is most probably associated with the directionality of the bonds and the symmetry of their orbitals. According to QTAIM and NBO analyses, H1 of **4** bears a small positive charge, while a negative charge (−0.34, QTAIM; −1.24, NBO) was found at C1. Therefore, one can consider the interaction between C1 and the C1′−H1 bond as a hydrogen bond donation from C1′−H1 of DME to the carbanionic center C1 of DMCA. Correspondingly, QTAIM and NBO analyses reveal that C2′−H4···C2 interaction can be regarded as a hydrogen bond. The hydrogen-bonding

(63) (a) Alkorta, I.; Rozas, I.; Elguero, J. *Chem. Soc. Rev.* **1998**, *27*, 163−170. (b) Braga, D.; De Leonardis, P.; Grepioni, F.; Tedesco, E.; Calhorda, M. J. *Inorg. Chem.* **1998**, *3337*, 7−3348. (c) Custelcean, R.; Jackson, J. E. *Chem. Rev.* **2001**, *101*, 1963−1980. (d) Maseras, F.; Lledós, A.; Clot, E.; Eisenstein, O. *Chem. Rev.* **2000**, *100*, 601−636. (e) Pakiari, A. H.; Mohajeri, A. *J. Mol. Struct. (THEOCHEM)* **2003**, *620*, 31−36. (f) Govender, M. G.; Ford, T. A. *J. Mol. Struct. (THEOCHEM)* **2003**, 11−16. (g) Crabtree, R. H.; Siegbahn, P. E. M.; Eisenstein, O.; Rheingold, A. L.; Koetzle, T. F. *Acc. Chem. Res.* **1996**, *29*, 348−354. (h) Belkova, N. V.; Besora, M.; Epstein, L. M.; Lledós, A.; Maseras, F.; Shubina, E. S. *J. Am. Chem. Soc.* **2003**, *125*, 7715−7725. (i) Shubina, E. S.; Belkova, N. V.; Krylov, A. N.; Vorontsov, E. V.; Epstein, L. M.; Gusev, D. G.; Niedermann, M.; Berke, H. *J. Am. Chem. Soc.* **1996**, *118*, 1105−1112. (j) Morrison, C. A.; Siddick, M. M. *Angew. Chem.* **2004**, *116*, 4884−4886; *Angew. Chem., Int. Ed.* **2004**, *43*, 4780−4782. (k) Richardson, T. B.; de Gala, S.; Crabtree, R. H.; Siegbahn, P. E. M. *J. Am. Chem. Soc.* **1995**, *117*, 12875−12876. (l) Cybulski, H.; Tyminska, E.; Sadlej, J. *ChemPhysChem* **2006**, *7*, 629−639. (m) Alkorta, I.; Elguero, J.; Foces-Foces, C. *Chem. Commun.* **1996**, 1633−1634. (n) Grabowski, S. J. *J. Phys. Chem. A* **2000**, *104*, 5551−5557. (o) Clement, N. D.; Cavell, K. J.; Jones, C.; Elsevier, C. J. *Angew. Chem.* **2004**, *116*, 1297−1299; *Angew. Chem., Int. Ed.* **2004**, *43*, 1277−1279.

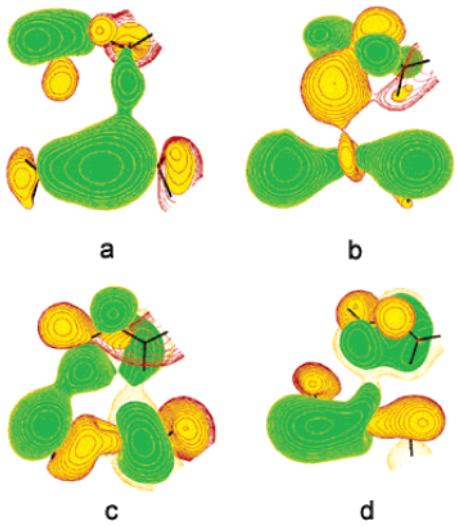

Figure 7. Contour maps of some MOs for the B3LYP/II-calculated DMCA−DME complex. The MO energies (E) are given in atomic units [au]: HOMO−3, $E = -0.0276$, contour value 0.03 (a); HOMO−4, $E = -0.0287$, contour value 0.016 (b); HOMO−7, $E = -0.126$, contour value 0.007 (c); HOMO−13, $E = -0.248$, contour value 0.01 (d).

Scheme 2. Bond (small filled circles) and Ring (small empty circles) Critical Points as Well as Bond Paths for a Hypothetical Trifurcated Hydrogen Bond between the C1′−H1 Bond of DME and the C(1)-Methyl Group in 4[65]

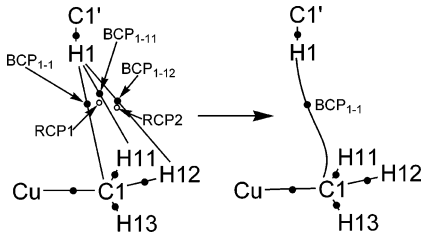

character of the above-described interaction of the C1−H11 and C1−H12 bonds with the C1′−H1 bond is supported by a decrease of electron densities at the respective atoms H11 and H12 in **4** compared with those in the unbound **1** (Table S4). The same is valid for atoms H21 and H22. Thus, according to QTAIM (Figure 6) and NBO theory, the interaction of the C1′−H1 bond of DME with the C(1)-methyl group of DMCA in **4** can be considered as a weak trifurcated hydrogen bond[63e,64] of C1′−H1 to the carbanionic center C1 and two hydridic atoms, H11 and H12, of DMCA. Three primary bond critical points (BCP_{1-1}, BCP_{1-11}, and BCP_{1-12}), two ring critical points (RCP1 and RCP2 of the three-membered rings H1−H11−C1 and H1−H12−C1), and the bond paths BP_{1-1}, BP_{1-11}, and BP_{1-12}, describing this trifurcated hydrogen bond, should occur in the very narrow space (Scheme 2, left side). As described for **2**, the closeness of atoms and critical points mentioned should result in the formation of new topologically unstable BCP_{1-1} and BP_{1-1}. The new BP_{1-1} should most probably deviate rather toward H11 and H12 (Scheme 2, right side) than toward the Cu−C1 bond,[66] as predicted for **4** (Figures 1 and 6). As in the case of complexes **2**, strong deviations of BP_{1-1} and BP_{4-2} toward the Cu−C1 and Cu−C2 bonds, respectively, are obviously due to appreciable interactions of the C1′−H1 and C2′−H4 bonds with Cu. Indeed, sufficiently strong back-donations from Cu to σ^*(C−H) and RY*(H) orbitals of the interacting C−H bonds of DME as well as second-order Cu−C→H−C orbital interactions exist as shown above. These donations stabilize **4** to an extent similar to interactions of C1′−H1 and C2′−H4 bonds with the methyl groups of DMCA (Table S5). Sufficiently strong interactions of C1′−H1 and C2′−H4 bonds with both the copper center and electron densities of C−Cu bonds in **4** lead, like a similar interaction of the C1′−H1 bond in complex **2d**, to a significant deviation of H1···C1 and H4···C2 bond paths toward Cu and the corresponding C−Cu bond. It is interesting to note that C1···H1 and C2···H4 separations of 2.817 Å in B3LYP/II-optimized **4** are equal to d(Cu−H1) in the MP2/II-optimized complex of DMCA with methane (**2c**). At the same time, Cu···H1 and Cu···H4 separations (2.904 Å) in **4** exceed d(Cu−H1) in **2c** by 0.04 Å. As was mentioned above, the structure **2c**, with the bond path linking the H1 and Cu and strongly deviating toward the C1−Cu bond, is topologically unstable. It can be easily transformed to a structure in which H1 is linked with the C1−Cu bond critical point to yield a "conflict structure",[15,51b] or a structure in which H1 is linked by a bond path with C1 (as in **2d**) or another (H11, H12) atom. The described data show that the lengthening of the Cu···H1 and Cu···H4 separations in **4** compared with the Cu···H1 distance in **2c** results in a structure in which the Cu···H1 and Cu···H4 bond paths are transformed to those linking H1 and H4 of DME with C1 and C2 of DMCA, respectively.

The discussion shows that the C1′−H1···C1 and C2′−H4···C2 interactions predicted for **4** by QTAIM are the multicenter-copper-assisted hydrogen bonds between C−H bonds of DME and DMCA according to NBO. Hence, a significant deviation of a bond path linking a particular C−H bond of a ligand with the carbanionic center of a diorganocuprate(I) anion toward the Cu−C bond is strong evidence for an interaction of that C−H bond with Cu and the C−Cu bond. Again, the $\nabla^2\rho_{BCP}$ value of 0.018 au for BCP_{1-1} and BCP_{4-2} in **4** is in the range determined for hydrogen bonds,[50,57b] and the positive and small H_{BCP} values calculated for BCP_{1-1} and BCP_{4-2} in **4** (Table S1) agree with those characterizing the closed-shell interactions including hydrogen bonds.[15,44,45b,50c,51]

Conclusions

The complexes of dimethylcuprate(I) anion (DMCA) with methane, propane, and dimethyl ether (DME) were theoretically studied using B3LYP and MP2 methods. The quantum theory of atoms in molecules (QTAIM) and the second-order perturbation NBO analyses were used for electron density distribution analysis and for the elucidation of the nature of weak closed-shell interactions of the ligands with DMCA. DMCA−methane, DMCA−propane, and DMCA−DME weak complexes were found to be real minima on the respective potential energy surfaces. From the dissociation energies of these complexes it was concluded that coordination of C−H bonds of ethereal solvents and crown ethers to diorganocuprate(I) anions is feasible.

The formation of C−H···Cu hydrogen bonds (HBs) was shown to be the most important factor stabilizing the calculated DMCA−methane and DMCA−propane complexes. In the formation of C−H···Cu hydrogen bonds, the copper atom bearing a partial positive charge acts as donor of electron charge to the C−H bonds. Such behavior of the copper atom of DMCA differs completely from that of bare Cu^+, which accepts electron

(64) Ranganathan, A.; Kulkarni, G. U.; Rao, C. N. R. *J. Phys. Chem. A* **2003**, *107*, 6073−6081.

(65) For the sake of clarity, the same picture for a hypothetical trifurcated hydrogen bond between C2′−H4 and the C(2)-methyl group is not shown here.

(66) This assumption is based on the analysis of reasons for the curving of bond paths described in the Appendix.

density mainly from C−H and other bonds and forms agostic complexes.[9,67]

In DMCA the presence of two methyl groups with negatively charged carbon atoms and hydridic hydrogens can lead additionally to the formation of C−H···C hydrogen and C−H···H−C dihydrogen bonds with C−H bonds of methane, propane, and DME. Such hydrogen-bonding interactions are predicted by NBO, molecular orbital analysis, and QTAIM analysis of envelopes of atomic basins. Second-order orbital interactions of C−Cu bonds with C−H bonds of methane, propane, and DME (Cu−C→H−C donor−acceptor interactions) also stabilize the complexes studied according to the second-order perturbation NBO analysis. This analysis predicts the formation of multicenter-copper-assisted hydrogen bonds with DMCA. Despite the complex nature of interactions in all complexes studied, there are only one or two bond paths linking hydrogen atoms of methane, propane, or DME with atoms of DMCA in the molecular graphs predicted by QTAIM. As a rule, these bond paths are strongly curved and deviate toward carbon−copper bonds, suggesting the interaction of C−H bonds of the ligands with electron densities of carbon−copper bonds. Such QTAIM description of the different closed-shell interactions in complexes of DMCA with methane, propane, and DME is explained by a coalescence of primary bond and ring critical points caused by their very similar properties. This QTAIM description is thus evidently different from the description by NBO.

According to the theoretical predictions of this work, C−H bonds of free ligands or ligands coordinated to a countercation of monomeric or dimeric diorganocuprate(I) can interact with diorganocuprate(I) anion and may affect the structure of highly flexible cuprate(I) aggregates. Indeed, QTAIM and NBO analyses, carried out on the X-ray structures of some monomeric diorganocuprates(I), reveal[68] that all predicted types of weak interactions do really exist in the solid-state structures of cuprates(I).

Binding energies calculated for model complexes noticeably increase on going from methane (0.4−1.1 kcal/mol) to propane (0.5−1.2 kcal/mol) and then to dimethyl ether (2.1−3.0 kcal/mol), i.e., on increasing the acidity of C−H bonds interacting with dimethylcuprate(I) anion. It is reasonable to propose that coordination of solvent molecules or molecules of other ligands to a cation (Li^+ as a rule) of a diorganocuprate(I) should enhance the acidity of C−H bonds of ligands and result in significantly larger binding energies of complexes of diorganocuprate(I) anions with the ligands. DFT calculations of monomeric lithium dimethylcuprate(I) solvated by three molecules of dimethoxyethane as well as some oligomers of this solvated dimethylcuprate(I) demonstrate that the energy of an interaction of dimethylcuprate(I) anion with ligands surrounding Li^+ can be as large as 10 kcal/mol, which can certainly affect the reactivity of a diorganocuprate(I). Results of these calculations will be published elsewhere. Ligands surrounding Li^+ form multiple hydrogen bonds with diorganocuprate(I) anions. This hydrogen-bonding interaction is accompanied by an unsymmetrical interaction of two parts of these anions with C−H bonds.[68] It could not be excluded that such unsymmetrical hydrogen-bonding interaction can lead also to a change in selectivity of diorganocuprates(I) with two different organic moieties.

The reasons why the bond paths in molecular graphs of the complexes studied are curved were analyzed. Such curved bond paths are observed in many other molecular systems described in the literature. The origin of the curving is likely to be the same for all types of closed-shell interactions such as hydrogen bond, agostic, and van der Waals interactions.

Acknowledgment. We gratefully acknowledge financial support from the Deutsche Forschungsgemeinschaft (Sonderforschungsbereich 260) and the Fonds der Chemischen Industrie. Also we thank the "Hochschulrechenzentrum der Philipps-Universität Marburg", the "Rechen- und Kommunikationszentrum der RWTH Aachen", and the "John von Neumann-Institut für Computing (NIC) in Jülich" for providing calculation time.

Appendix

Reasons of Bond Path Curvatures. Curving of bond paths linking atoms of C−H bonds of methane, propane, and DME with atoms of DMCA (Figure 1) is not a unique phenomenon and previously has also been observed for other hydrogen-bonded systems[50b,d,64,67,69] for complexes of Cu(I),[9] other transition metals,[52,53c,70,71] and different weakly bonded complexes.[51b,70,72] The curved metal−carbon bond paths were revealed for some 3d metal metallocenes[73] and ethylenebis(indenyl-1)zirconium dichloride.[74] Also significantly curved metal−carbon and metal−metal bond paths were computed for transition metal carbonyl clusters[26b,75a] and for three-membered rings of bis(1,5-cyclooctadiene)nickel.[75b] For $[Ni(H_3L)][NO_3][PF_6]$ [H_3L = *N*,*N*′,*N*″-tris(2-hydroxy-3-methylbutyl)-1,4,7-triazacyclononane] a strongly curved Ni−O bond path is observed, whereas the Ni−N bond path is almost linear.[76] Thus, a curvature of the bond path is not an exclusive characteristic of β-agostic alkyls of the early transition metals[77] and cannot be used to distinguish agostic interactions from classical hydrogen bonds, as was supposed recently.[77] To understand general reasons of bond path curvatures, let us consider second-order orbital interactions between closed-shell molecules AB and XY shown in Scheme 3. The same results will be obtained if the QTAIM approach is applied with respect to closed-shell interactions[15,44,45b,50c,51,53a] between molecules AB and XY. The analysis of the literature data cited above and results of this work show that a significant curving of a bond path between the atoms B and X seems to occur if the A−B···X angle (φ(A−B···X)) decreases to about 120° or further. Such a decrease of φ(A−B···X) may be caused by

(67) Alcamí, M.; Luna, A.; Mó, O.; Yáñez, M.; Tortajada, J. *J. Phys. Chem. A* **2004**, *108*, 8367−8372.

(68) Dem′yanov, P. I.; Gschwind, R. M., to be published.

(69) (a) Popelier, P. L. A.; Bader, R. F. W. *Chem. Phys. Lett.* **1992**, *189*, 542−548. (b) Rozas, I.; Alkorta, I.; Elguero, J. *J. Phys. Chem. A* **1997**, *101*, 9457−9463. (c) Znamenskiy, V. S.; Green, M. E. *J. Phys. Chem. A* **2004**, *108*, 6543−6553. (d) Palusiak, M.; Grabowski, S. J. *J. Mol. Struct. (THEOCHEM)* **2004**, *674*, 147−152. (e) DuPré, D. B. *J. Phys. Chem. A* **2005**, *109*, 622−628.

(70) Popelier, P. L. A.; Logothetis, G. *J. Organomet. Chem.* **1998**, *555*, 101−111.

(71) Scherer, W.; Hieringer, W.; Spiegler, M.; Sirsch, P.; McGrady, G. S.; Downs, A. J.; Haaland, A.; Pedersen, B. *Chem. Commun.* **1998**, 2471−2472.

(72) (a) Popelier, P. L. A. *J. Phys. Chem. A* **1998**, *102*, 1873−1878. (b) Cioslowski, J.; Mixon, S. T. *Chem. Phys. Lett.* **1990**, *170*, 297−300. (c) Cioslowski, J.; Mixon, S. T.; Edwards, W. D. *J. Am. Chem. Soc.* **1991**, *113*, 1083−1085.

(73) Lyssenko, K. A.; Golovanov, D. G.; Antipin, M. Y. *Mendeleev Commun.* **2003**, 209−211.

(74) Stash, A. I.; Tanaka, K.; Shiozawa, K.; Makino, H.; Tsirelson, V. G. *Acta Crystallogr.* **2005**, *B61*, 418−428.

(75) (a) Macchi, P.; Garlaschelli, L.; Sironi, A. *J. Am. Chem. Soc.* **2002**, *124*, 14173−14184. (b) Macchi, P.; Proserpio, D. M.; Sironi, A. *J. Am. Chem. Soc.* **1998**, *120*, 1447−1455.

(76) Smith, G. T.; Mallinson, P. R.; Frampton, C. S.; Farrugia, L. J.; Peacock, R. D.; Howard, J. A. K. *J. Am. Chem. Soc.* **1997**, *119*, 5028−5034.

(77) Scherer, W.; McGrady, G. S. *Angew. Chem.* **2004**, *116*, 1816−1842; *Angew. Chem., Int. Ed.* **2004**, *43*, 1782−1806.

Scheme 3. Molecular (1), Orbital (2), and Topological (3) Representations of Hypothetical Transformations of End-On into Side-On Interactions of Orbitals of Atom X in Molecule XY with Orbitals of Molecule AB[a] [78]

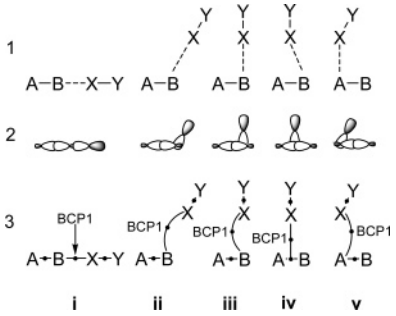

[a] In line 3, the small filled circles on the bond paths linking two interacting atoms are bond critical points.

geometrical and/or electronic requirements, with the latter resulting in an increased energy of the X···B interaction. With the decrease of φ(A−B···X) to 120° and farther, orbitals of atom X as well as those of the bond X−Y located closer to or mainly on atom X should interact increasingly with orbitals located between A and B, whereas their interaction with those orbitals located mainly on the outer part of atom B should decrease. In other words, the end-on mode of interactions of atom X and bond X−Y with the A−B bond in structure **i** changes appreciably to a side-on mode in structures **ii** and **iii** (Scheme 3, line 1). On moving the interaction domain of atom X and bond X−Y along the B−A bond, an atomic interaction line (bond path for a stable [(A−B)·(X−Y)] complex) between atoms X and B (BP_{XB}), a line along which the electron density is maximal with respect to any neighboring line in the space defined by A, B, and X, will be displaced from B to A and bend increasingly toward bond path BP_{AB} linking atoms A and B, as shown in line 3 of Scheme 3. Consequently, BCP1 associated with BP_{XB} will be shifted from its position in **i** to that in **ii** and **iii**. Such changes occur on going from **2a** to **2b** and to **2c**. If the charge transfer interaction domains of orbitals of atom X and bond X−Y with orbitals of the A−B bond move closer to atom A, at first the BP_{XB} switches from atom B in **i**, **ii**, and **iii** to the bond critical point of the A−B bond in **iv**. This transformation leads to structures described by the conflict molecular graph[15] **iv** (Scheme 3, line 3) or the conflict structures of the van der Waals complexes Ar···C_2H_2, Ar···CO_2, and Ar···COS.[51b] It should be noted that the molecular graph of **2c** is close to a conflict structure. Then, the structure described by molecular graph **v**, similar to that predicted for complex **2d**, is formed. In this structure the orbitals of atom X and bond X−Y interact with those orbitals of the A−B bond located closer to atom A as well as those located on atom A itself. Further moving along the B−A bond may finally result in switching the interaction to atom A, i.e., lead to the formation of the end-on Y−X···A−B complex (not shown in Scheme 3).

If in a molecule BA−S−YX with spacer S there is an intramolecular closed-shell[15,44,45b,50c,53a] (noncovalent) interaction of atom X with atom B and/or an end-on interaction with the A−B bond via its B terminus, a cyclic structure **c1** described by molecular graph **j** (Scheme 4) is formed. Let us consider what happens if a decrease of the A−B···X angle takes place due to some reason. This decrease can lead to switching of second-order charge transfer interactions of orbitals of atom X, and possibly bond X−Y orbitals located closer to atom X, to the interactions with orbitals of the A−B bond only. In the molecular graph **j** for the cycle **c1**, this will lead both to a

Scheme 4. Molecular (1), Orbital (2), and Topological (3) Representations of Hypothetical Intramolecular Transformations of End-On into Side-On Interactions of Atom X Orbitals in Molecule BA−S−YX with A−B Bond Orbitals[a] [78]

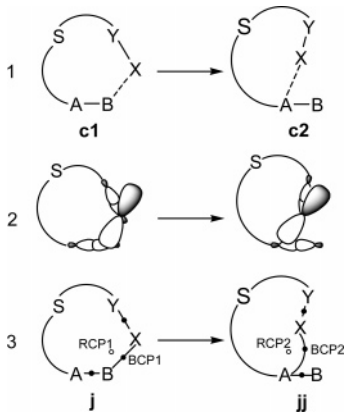

[a] In line 3, the small filled circles on the bond paths linking interacting atoms and the small open cycles are bond and ring critical points, respectively.

deviation of the lower terminus of the BP_{BX}, which links atoms B and X, to the A−B bond and to a shift of this BP as a whole toward atom A. BCP1 associated with the BP_{BX} would subsequently shift toward the RCP1 as a result of these changes. In further displacement of the X···B−A interaction domain along the B−A bond toward atom A, a coalescence[15,50c,51b] of the BCP1 and RCP1 occurs, which results in the formation of a new BCP2 between A and X, a new BP_{AX}, linking A and X, and a new RCP2 (Scheme 4, right side). As a result, the structure **c2** described by the molecular graph **jj** will be formed. It is notable that similar changes in molecular graphs were described for three-membered C−TM−C (TM is a transition metal atom) rings[75b] and for $[FeCo(CO)_8]^-$ upon changing the Fe−Co−C angle along the terminal to bridging conversion path.[26b,75]

The general considerations described here allow one to establish a rationale for the curved bond paths in **2**, **3**, and **4**, which are results of multicenter side-on interactions of C−H bonds of methane, propane, and DME with DMCA. It should be pointed out that the changes in structures and molecular graphs described were not associated with the particular type of second-order (noncovalent) orbital interactions of atom X and/or bond X−Y with atom B and/or A−B bond. Hence these changes are obviously applicable equally to all so-called closed-shell interactions, i.e., noncovalent interactions such as ionic bonds, hydrogen bonds including those formed with transition metal atoms,[2,4] van der Waals[41d,51b] and hydrogen−hydrogen[50c,61] interactions, agostic interactions,[2,3,77,79] and formation of σ-complexes.[1f,h]

Supporting Information Available: Properties of bond critical points; QTAIM and NBO charges of the individual atoms of the dimethylcuprate anion and the complexes studied; changes in QTAIM and NBO electron populations of the atoms in the complexes with respect to those in the respective free reactants; data on selected second-order donor−acceptor orbital interactions in the complexes; delocalization indices for the complexes. This material is available free of charge via the Internet at http://pubs.acs.org.

OM0604066

(78) In line 2, only one of these interactions, namely, an interaction of the LP orbital of atom X with the A−B bond orbital, is demonstrated for simplicity.

(79) Baratta, W.; Mealli, C.; Herdtweck, E.; Ienco, A.; Mason, S. A.; Rigo, P. *J. Am. Chem. Soc.* **2004**, *126*, 5549−5562.